Inorganic Chemistry

Article

pubs.acs.org/IC

Metal Azolate/Carboxylate Frameworks as Catalysts in Oxidative and C−C Coupling Reactions

Aurel Tăbăcaru,[†] Nertil Xhaferaj,[‡] Luísa M. D. R. S. Martins,[*,§,∥] Elisabete C. B. A. Alegria,[§,∥] Rogério S. Chay,[∥] Carlotta Giacobbe,[⊥,#] Konstantin V. Domasevitch,[¶] Armando J. L. Pombeiro,[*,∥] Simona Galli,[*,⊥] and Claudio Pettinari[*,‡]

[†]Department of Chemistry, Physics and Environment, Faculty of Sciences and Environment, "Dunarea de Jos" University of Galati, 111 Domneasca Street, 800201 Galati, Romania

[‡]School of Pharmacy, Chemistry Section, University of Camerino, Via S. Agostino 1, 62032 Camerino, Italy

[§]Chemical Engineering Department, Instituto Superior de Engenharia de Lisboa, Instituto Politécnico de Lisboa, R. Conselheiro Emídio Navarro, 1959-007 Lisboa, Portugal

[∥]Centro de Química Estrutural, Instituto Superior Técnico, Universidade de Lisboa, Avenida Rovisco Pais, 1049-001 Lisboa, Portugal

[⊥]Dipartimento di Scienza e Alta Tecnologia, Università dell'Insubria, Via Valleggio 11, 22100 Como, Italy

[#]ID22 High-Resolution Powder-Diffraction Beamline, European Synchrotron Radiation Facility, CS 40220, 38043 Grenoble Cedex 9, France

[¶]National Taras Shevchenko University of Kyiv, Volodimirska Strasse 64, 01033 Kyiv, Ukraine

Supporting Information

ABSTRACT: The five metal azolate/carboxylate (MAC) compounds [Cd(dmpzc)(DMF)(H_2O)] (**Cd-dmpzc**), [Pd(H_2dmpzc)$_2$$Cl_2$] (**Pd-dmpzc**), [Cu(Hdmpzc)$_2$] (**Cu-dmpzc**), [Zn_4O(dmpzc)$_3$]·Solv (**Zn-dmpzc·S**), and [Co_4O(dmpzc)$_3$]·Solv (**Co-dmpzc·S**) were isolated by coupling 3,5-dimethyl-1*H*-pyrazol-4-carboxylic acid (H_2dmpzc) to cadmium(II), palladium(II), copper(II), zinc(II), and cobalt(II) salts. While **Cd-dmpzc** and **Pd-dmpzc** had never been prepared in the past, for **Cu-dmpzc**, **Zn-dmpzc·S**, and **Co-dmpzc·S** we optimized alternative synthetic paths that, in the case of the copper(II) and cobalt(II) derivatives, are faster and grant higher yields than the previously reported ones. The crystal structure details were determined ab initio (**Cd-dmpzc** and **Pd-dmpzc**) or refined (**Cu-dmpzc**, **Zn-dmpzc·S**, and **Co-dmpzc·S**) by means of powder X-ray diffraction (PXRD). While **Cd-dmpzc** is a nonporous 3D MAC framework, **Pd-dmpzc** shows a 3D hybrid coordination/hydrogen-bonded network, in which Pd(H_2dmpzc)$_2$$Cl_2$ monomers are present. The thermal behavior of the five MAC compounds was investigated by coupling thermal analysis to variable-temperature PXRD. Their catalytic activity was assessed in oxidative and C−C coupling reactions, with the copper(II) and cadmium(II) derivatives being the first nonporous MAC frameworks to be tested as catalysts. **Cu-dmpzc** is the most active catalyst in the partial oxidation of cyclohexane by *tert*-butyl hydroperoxide in acetonitrile (yields up to 12% after 9 h) and is remarkably active in the solvent-free microwave-assisted oxidation of 1-phenylethanol to acetophenone (yields up to 99% at 120 °C in only 0.5 h). On the other hand, activated **Zn-dmpzc·S** (**Zn-dmpzc**) is the most active catalyst in the Henry C−C coupling reaction of aromatic aldehydes with nitroethane, showing appreciable diastereoselectivity toward the *syn*-nitroalkanol isomer (syn:anti selectivity up to 79:21).

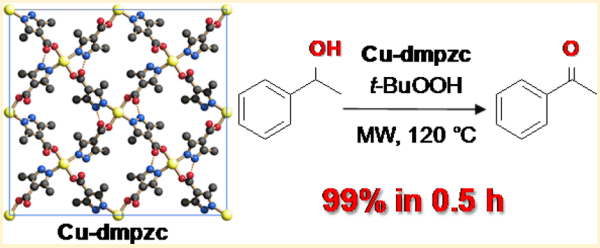

1. INTRODUCTION

The enormous fields of coordination polymers (CPs)[1] and metal−organic frameworks (MOFs)[2] have been unexhaustively developing because of their potential use in a wide range of key functional applications, spanning from luminescence to magnetism, gas storage, gas or liquid separation, drug delivery, and imaging, to mention only a few. Heterogeneous catalysis is another, industrially relevant application for which CPs[3] and MOFs[4] have shown promising performances, emerging as versatile alternatives to the traditional all-inorganic materials for a number of organic syntheses. Indeed, CPs and MOFs couple the periodic organization of catalytically active centers (the metal nodes) to a convenient modulation of the catalytic performances through the electronic and steric properties of the spacers. To these aspects, when size and shape selectivity are required, MOFs add homogeneous pore-size and pore-wall decoration.

A crucial aspect potentially hampering the implementation of CPs and MOFs into real-world applications is their chemical and thermal stability. Poly(carboxylato)-based MOFs, the first class of MOFs to be systematically explored, have shown

Received: January 2, 2016

DOI: 10.1021/acs.inorgchem.5b02997
Inorg. Chem. XXXX, XXX, XXX−XXX

interesting functional properties, yet, on some occasions, they have shown a limited stability to hydrolysis,[5] hampering their use at the industrial level.

Poly(azolate) ligands, generally granting stronger metal-to-ligand coordinative bonds compared to their oxygen-donor counterparts, have been exploited more recently as a means to improve the chemical and thermal stability of the resulting coodination compounds.[6] The interested reader can find in ref 7 a comprehensive review of the most recent advances achieved in the field of metal azolate frameworks, from the points of view of crystal engineering and functional properties. In the past years, we have been focusing on the preparation of rigid and flexible poly(pyrazole) ligands, with the final aim of building up CPs and MOFs characterized by remarkable thermal robustness[8] and chemical stability toward harsh conditions.[9] Besides these aspects, poly(pyrazolato)-containing CPs and MOFs typically possess interesting crystal structures and functional properties.[10]

More recently, a limited number of metal azolate/carboxylate (MAC) frameworks,[11] built up with pyrazolate-,[11,12] triazolate-,[13] tetrazolate-,[14] or imidazolate/carboxylate[15] spacers, have appeared in the literature.

To the best of our knowledge, $NH_4[Cu_3(\mu_3\text{-}OH)(\mu_3\text{-}4\text{-carboxypyrazolato})_3]$[12a] is the only MAC framework ever tested as a catalyst, namely, in the oxidation of cyclohexane (CyH) and cyclohexene with *tert*-butyl hydroperoxide. Aiming at enlarging the family of MAC compounds essayed as catalysts, we focused our attention on 3,5-dimethyl-1*H*-pyrazol-4-carboxylic acid (H_2dmpzc, Scheme 1). This spacer has already been employed successfully in the recent past: the MOF $[Cu_2(dmpzc)_2(H_2O)]\cdot 1.5DMF$ (DMF = *N*,*N*-dimethylformamide) has shown selective adsorption of C_2H_2 versus C_2H_4, C_2H_6, and CO_2 in the low-pressure range ($P < 10$ kPa) and a very high selectivity toward C_2H_2, C_2H_4, C_2H_6, and CO_2 with respect to CO or N_2.[12c] After thermal activation, when probed with CO_2 and CH_4, the MOFs $[M_4(O)(dmpzc)_3]\cdot Solv$ [M = Zn (**Zn-dmpzc·S**),[11,12a] Co (**Co-dmpzc·S**)[11]], undergo guest-induced gate opening. More interestingly, the cobalt(II) derivative adsorbs up to 20.8 wt % CO_2 at 273 K and 1 bar,[11] while the zinc(II) compound selectively captures harmful volatile organic compounds, even in competition with moisture.[12b] At 10 K and under a static field of 5 kOe, $[Cu(Hdmpzc)_2]$ (**Cu-dmpzc**) is dominated by antiferromagnetic interactions.[12d] Finally, $[Cr_3O(Hdmpzc)_6(DMF)_3]$ adsorbs up to 57 mL/g of CO_2 at 100 kPa.[12f]

Scheme 1. Molecular Structure of H_2dmpzc

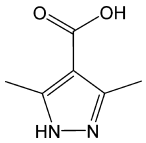

In the present work, we isolated and characterized two novel MAC compounds, namely, $[Cd(dmpzc)(DMF)(H_2O)]$ (**Cd-dmpzc**) and $[Pd(H_2dmpzc)_2Cl_2]$ (**Pd-dmpzc**). For our catalytic tests, we adopted **Cd-dmpzc** and **Cu-dmpzc** as representatives of the class of 3D nonporous MAC frameworks and **Pd-dmpzc** as an example of a 3D hybrid coordination/hydrogen-bonded network. Finally, repeatedly failing at isolating novel derivatives having the M(dmpzc) formula with M = Zn and Co, we selected **Zn-dmpzc·S** and **Co-dmpzc·S** as members of the class of 3D porous MAC frameworks to be thermally activated and essayed. In the following, the results of our catalytic tests in oxidative and C−C coupling reactions are reported and discussed.

2. EXPERIMENTAL SECTION

2.1. Materials and Methods. All chemicals and reagents were purchased from Sigma-Aldrich Co. and used as received, without further purification. All solvents were distilled prior to use following consolidated procedures.[16] Before the analytical characterization was performed, all samples were dried in vacuo (50 °C, ∼0.1 Torr) until a constant weight was reached. The IR spectra were recorded from 4000 to 650 cm^{-1} with a PerkinElmer Spectrum 100 instrument by attenuated total reflectance (ATR) on a CdSe crystal. Elemental analyses (carbon, hydrogen, and nitrogen) were performed with a Fisons Instruments 1108 CHNS-O elemental analyzer. Thermogravimetric analyses (TGAs) were carried out under a N_2 flow with a PerkinElmer STA 6000 simultaneous thermal analyzer with a heating rate of 7 °C/min. ^{1}H NMR spectra were recorded at ambient temperature on a Bruker Avance II + 300 (UltraShield Magnet) spectrometer operating at 300 MHz. In the following, the chemical shifts are reported in ppm, using tetramethylsilane as the internal reference.

2.2. Synthesis of H_2dmpzc. H_2dmpzc was synthesized by following a previously reported procedure.[11] Elem anal. Calcd for $C_6H_8N_2O_2$ (fw = 140.14 g/mol): C, 51.42; H, 5.75; N, 19.99. Found: C, 51.11; H, 5.63; N, 19.45. Mp: 295−300 °C (dec). IR (ATR, cm^{-1}): 3192 (w, br); 2932 (w, br); 2516 (m, br); 1669 (s); 1566 (m); 1505 (s); 1422 (s); 1320 (s); 1272 (s); 1122 (s); 1054 (m); 992 (m); 917 (m); 760 (s). ^{1}H NMR (DMSO, 298 K): δ 2.29 (s, 6H, CH_3), 12.3 (s, COO*H*).

2.3. Synthesis of [Cd(dmpzc)(DMF)(H_2O)] (Cd-dmpzc). H_2dmpzc (0.07 g, 0.5 mmol) was dissolved in DMF (15 mL); after complete dissolution, $Cd(CH_3COO)_2\cdot 2H_2O$ (0.15 g, 0.5 mmol) was added. The mixture was left under stirring in a high-pressure glass tube at 150 °C for 24 h, until a white precipitate formed. The latter was filtered off, washed with DMF (2 × 10 mL), and dried in vacuo. Yield: 68%. **Cd-dmpzc** is insoluble in alcohols, dimethyl sulfoxide (DMSO), DMF, acetone, acetonitrile (MeCN), chlorinated solvents, and water (H_2O). Elem anal. Calcd for $C_9H_{15}CdN_3O_4$ (fw = 341.64 g/mol): C, 31.64; H, 4.42; N, 12.30. Found: C, 31.29; H, 4.12; N, 11.95. IR (ATR, cm^{-1}): 3329 (w, br) ν(O−H_{water}); 3000−2900 (w) ν(C−$H_{aliphatic}$); 1664 (s); 1655 (s) ν(C═O_{DMF}); 1549 (vs); 1509 (vs) ν_{asym}(COO^-); 1419 (vs); 1396 (vs); 1376 (vs) ν_{sym}(COO^-); 1167 (vs); 1112 (m); 1064 (w); 1014 (w); 990 (w); 935 (w); 838 (s); 824 (s); 805 (s); 682 (s); 666 (s).

2.4. Synthesis of [Pd(H_2dmpzc)$_2$$Cl_2$] (Pd-dmpzc). H_2dmpzc (0.07 g, 0.5 mmol) was dissolved in methanol (MeOH; 5 mL); after complete dissolution, $Pd(CH_3CN)_2Cl_2$ (0.13 g, 0.5 mmol) was added. A yellow suspension was formed and left overnight under stirring at room temperature. The yellow precipitate was filtered off, washed with MeOH (3 × 5 mL), and dried in vacuo. Yield: 61%. **Pd-dmpzc** is soluble in DMSO and DMF, while it is insoluble in alcohols, acetone, MeCN, chlorinated solvents, and water. Elem anal. Calcd for $C_{12}H_{16}Cl_2N_4O_4Pd$ (fw = 457.61 g/mol): C, 31.49; H, 3.52; N, 12.24. Found: C, 30.96; H, 3.24; N, 11.86. IR (ATR, cm^{-1}): 3195 (m, br) ν(N−H); 3200−2400 (br); 1683 (vs) ν(C═O); 1571 (m); 1521 (s) ν(C═C+C═N); 1148 (vs); 1036 (w); 921 (s); 776 (s).

2.5. Synthesis of [Cu(Hdmpzc)$_2$] (Cu-dmpzc). **Cu-dmpzc** was previously isolated in the form of single crystals with 40% yield by following a 3-day synthetic path.[12d] No mention was made by Qi and co-workers of an alternative method to isolate bulk powders. Here we propose a faster, 1-day procedure to obtain **Cu-dmpzc** in the form of polycrystalline powders with a higher yield. H_2dmpzc (0.07 g, 0.5 mmol) and $Cu(CH_3COO)_2$ (0.09 g, 0.5 mmol) were added to distilled water (10 mL). The mixture was left overnight at reflux under stirring: a brown suspension was formed. Upon cooling of the solution to room temperature, a violet precipitate was eventually formed. The latter was filtered off, washed with distilled water (2 × 10 mL), and dried in

DOI: 10.1021/acs.inorgchem.5b02997
Inorg. Chem. XXXX, XXX, XXX−XXX

vacuo. Yield: 55%. **Cu-dmpzc** is insoluble in alcohols, acetone, MeCN, DMF, DMSO, chlorinated solvents, and water. Elem anal. Calcd for $C_{12}H_{14}CuN_4O_4$ (fw = 341.81 g/mol): C, 42.17; H, 4.12; N, 16.39. Found: C, 42.27; H, 4.28; N, 15.94. IR (ATR, cm^{-1}): 3170 (m) ν(N−H); 3000−2900 (w) ν(C−$H_{aliphatic}$); 1585 (vs) ν_{asym}(COO^-); 1518 (m) ν(C=C+C=N); 1373 (s) ν_{sym}(COO^-); 1308 (m); 1179 (s); 1161 (s); 1073 (m); 825 (m); 808 (m); 787 (m); 753 (vs).

2.6. Synthesis of $[Zn_4O(dmpzc)_3]\cdot 2DMF\cdot 5H_2O$ (Zn-dmpzc·S). **Zn-dmpzc·S** was previously synthesized either in the form of bulk powders[12b] or as single crystals.[11] Here we propose an alternative synthetic path, which was originally implemented by us to obtain a coordination compound having the formula Zn(dmpzc): H_2dmpzc (0.07 g, 0.5 mmol) was dissolved in DMF (5 mL); after complete dissolution, $Zn(NO_3)_2\cdot 6H_2O$ (0.12 g, 0.5 mmol) was added. The solution was left under stirring in a high-pressure glass tube at 120 °C for 1 day. The resulting white precipitate was filtered off, washed with warm DMF (2 × 5 mL), and dried in vacuo. Yield: 75%. **Zn-dmpzc·S** is insoluble in alcohols, DMSO, DMF, acetone, MeCN, chlorinated solvents, and water. Elem anal. Calcd for $C_{24}H_{42}N_8O_{14}Zn_4$ (fw = 928.15 g/mol): C, 31.05; H, 4.56; N, 12.07. Found: C, 31.21; H, 4.45; N, 11.73. IR (ATR, cm^{-1}): 3000−2900 (w) ν(C−$H_{aliphatic}$); 1678 (s) ν(C=O_{DMF}); 1517 (vs); 1491 (vs) ν_{asym}(COO^-); 1428 (vs); 1407 (vs); 1377 (vs) ν_{sym}(COO^-); 1182 (vs); 1090 (m); 995 (m); 821 (s); 804 (s); 658 (m).

2.7. Synthesis of $[Co_4O(dmpzc)_3]\cdot 4DMF\cdot H_2O$ (Co-dmpzc·S). **Co-dmpzc·S** was previously synthesized in the form of single crystals with 60% yield by following a 3-day synthetic path.[11] No mention was made by Heering and co-workers of a method to isolate bulk powders. Here we propose a 2-day procedure, which was originally implemented by us to obtain a coordination compound having the formula Co(dmpzc), allowing us to isolate **Co-dmpzc·S** in the form of polycrystalline powders with a higher yield: H_2dmpzc (0.07 g, 0.5 mmol) was dissolved in DMF (5 mL); after complete dissolution, $Co(NO_3)_2\cdot 6H_2O$ (0.12 g, 0.5 mmol) was added. The solution was left under stirring in a high-pressure glass tube at 120 °C for 2 days. The resulting dark-blue precipitate was filtered off, washed with warm DMF (2 × 5 mL), and dried in vacuo. Yield: 65%. **Co-dmpzc·S** is insoluble in alcohols, DMSO, DMF, acetone, MeCN, chlorinated solvents, and water. Elem anal. Calcd for $C_{30}H_{48}Co_4N_{10}O_{12}$ (fw = 976.49 g/mol): C, 36.90; H, 4.95; N, 14.34. Found: C, 37.23; H, 4.62; N, 13.96. IR (ATR, cm^{-1}): 3000−2900 (w) ν(C−$H_{aliphatic}$); 1657 (s) ν(C=O_{DMF}); 1515 (vs); 1486 (vs) ν_{asym}(COO^-); 1424 (vs); 1404 (vs); 1373 (vs) ν_{sym}(COO^-); 1179 (vs); 1091 (m); 991 (m); 820 (s); 800 (s); 659 (m).

2.8. Powder X-ray Diffraction (PXRD) Crystal Structure Determination or Refinement. Polycrystalline samples of **M-dmpzc** (M = Cd, Pd, Cu) and **M-dmpzc·S** (M = Zn, Co) were gently ground in an agate mortar. Then, they were deposited in the hollow of a silicon zero-background plate. Diffraction data were collected at room temperature by means of overnight scans in the 2θ range of 5−105°, with steps of 0.02°, on a Bruker AXS D8 Advance diffractometer, equipped with nickel-filtered Cu Kα radiation (λ = 1.5418 Å), a Lynxeye linear position-sensitive detector, and the following optics: primary beam Soller slits (2.3°); a fixed divergence slit (0.5°); a receiving slit (8 mm). The generator was set at 40 kV and 40 mA. For **Cd-dmpzc** and **Pd-dmpzc**, a standard peak search, followed by indexing through the Singular Value Decomposition approach,[17] implemented in *TOPAS-R*,[18] allowed us to retrieve their approximate unit cell parameters. The space groups were assigned on the basis of the systematic absences. Structure solutions were performed by the simulated annealing method, implemented in *TOPAS-R*, employing a rigid, idealized models for the crystallographic independent portion of the ligand and DMF.[19] When viable, the torsion angle around the C−COO(H) bond was allowed to refine. The final refinements were carried out by the Rietveld method, maintaining the idealized models used at the solution stage. With regard to **Cu-dmpzc**, **Zn-dmpzc·S**, and **Co-dmpzc·S**, Rietveld refinements were carried out starting from the available structural information in refs 12d, 11, and 11, respectively. Because the atom-by-atom approach is unfeasible in PXRD, in all cases, the ligand was described as a rigid group[19] and its degrees of freedom (position of the center of mass, orientation within the unit cell) were refined. In the case of **Cu-dmpzc**, the starting point was a single-crystal structure determination *at 150 K*:[12d] our refinement from PXRD data collected *at room temperature* highlights the feasibility of obtaining the main structural details even without resorting to unconventional experimental conditions (e.g., the N_2 flow necessary to maintain the single crystal at 150 K). In all cases, the peak shapes were described with the fundamental parameters approach.[20] In the case of **Pd-dmpzc** and **Cu-dmpzc**, the peak-shape anisotropy was modeled with the aid of spherical harmonics. The background was modeled by a polynomial function. One, refined, isotropic thermal parameter was assigned to the metal atoms (B_M), with lighter atoms being given a $B = B_M + 2.0$ Å^2 value. The final Rietveld refinement plots for **Cd-dmpzc**, **Cu-dmpzc**, and **Pd-dmpzc** are collectively supplied in Figure S1. Fractional atomic coordinates are provided in the Supporting Information as CIF files. CCDC 1444441−1444443 contain the supplementary crystallographic data for **Cd-dmpzc**, **Cu-dmpzc**, and **Pd-dmpzc**, respectively. The data can be obtained free of charge from The Cambridge Crystallographic Data Centre via www.ccdc.cam.ac.uk/structures.

2.9. Variable-Temperature Powder X-ray Diffraction (VT-PXRD). To complement the TGAs, the thermal behavior of the **M-dmpzc** (M = Cd, Pd, Cu) and **M-dmpzc·S** (M = Zn, Co) materials was investigated by VT-PXRD.[21] As a first experiment, the cadmium(II), palladium(II), copper(II), and cobalt(II) derivatives were heated in air from 30 °C up to decomposition, with steps of 20 °C; a PXRD pattern was acquired at each step, covering a sensible low-to-medium-angle 2θ range, using a custom-made sample heater (Officina Elettrotecnica di Tenno, Ponte Arche, Italy). Treating the data acquired before loss of crystallinity by means of a Le Bail parametric refinement allowed us to disclose the behavior of the unit cell parameters as a function of the temperature. A VT-PXRD characterization of **Zn-dmpzc·S**, from 30 °C up to decomposition, was carried out by some of us in the recent past,[12b] and, consequently, it was not repeated in the present work. As a second experiment, in order to evaluate their reusability, the **M-dmpzc** (M = Cd, Pd, Cu) and **M-dmpzc·S** (M = Zn, Co) compounds were monitored by PXRD during five heating−cooling cycles, in air, in the range of 30−150 °C. The upper limit of the temperature range was chosen in view of the conditions adopted for the catalytic tests (see section 2.10).

2.10. Catalysis. *2.10.1. Peroxidative Oxidation of CyH with t-BuOOH.* The oxidation reactions of CyH were typically carried out in air, in thermostated Pyrex cylindrical vessels or round-bottom flasks, under vigorous stirring, and using MeCN as the solvent (total volume of up to 5.0 mL). In a typical experiment, **M-dmpzc** and, in selected occasions, trifluoroacetic acid (TFA), were added to MeCN together with CyH and the gas chromatography (GC) internal standard ($MeNO_2$, 0.05 mL). In the experiments carried out in the presence of radical traps, either $CBrCl_3$ (2.3 mmol) or $NHPh_2$ (2.3 mmol) was added to the reaction mixture. The reaction was started upon the addition of *t*-BuOOH (aqueous, 70%). Concentrations in the reaction mixture were as follows: **M-dmpzc** (2.5−10 μmol, 0.1−0.5 mol % vs substrate), TFA (5×10^{-3} M), CyH (0.46 M), and *t*-BuOOH (0.56 M). The reaction mixture was vigorously stirred at 50 °C for 0.5−12 h; aliquots of the reaction mixture were taken during the reaction and analyzed by GC. Before GC analysis was performed, an excess of triphenylphosphine was added to the aliquot, following a method developed by Shul'pin,[22] in order to reduce both the residual *t*-BuOOH and the alkyl peroxides that are formed as major products in alkane oxidations. GC measurements were carried out using a FISONS Instruments GC 8000 series gas chromatograph, equipped with a flame ionization detector, a DB-WAX capillary column (length = 30 m; internal diameter = 0.32 mm), and helium as the carrier gas, and run by the Jasco-Borwin version 1.50 software. The temperature of the injection was 240 °C. The column was initially maintained at 100 °C for 1 min, and then it was heated up to 180 °C with steps of 10 °C/min and held at this temperature for 1 min. The attribution of the observed GC peaks was carried out on the basis of chromatograms acquired on pure cyclohexanol (CyOH) and cyclohexanone (CyO) samples. Besides that, calibration curves were obtained with known

DOI: 10.1021/acs.inorgchem.5b02997
Inorg. Chem. XXXX, XXX, XXX−XXX

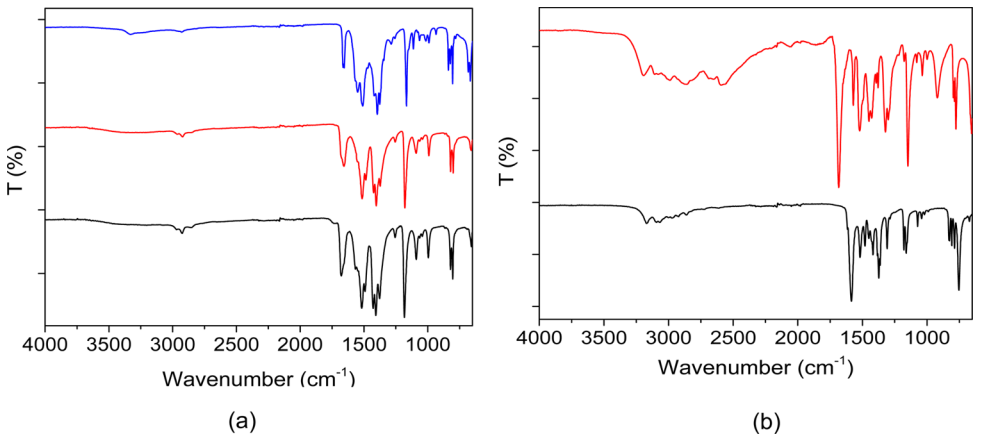

Figure 1. (a) Fourier transform infrared spectra of **Cd-dmpzc** (blue), **Zn-dmpzc·S** (black), and **Co-dmpzc·S** (red). (b) Fourier transform infrared spectra of **Pd-dmpzc** (red) and **Cu-dmpzc** (black).

concentrations of samples of pure products and standard. A number of blank experiments, performed in the absence of **M-dmpzc** by varying the amount of *t*-BuOOH and the other reagents, confirmed that no product of CyH oxidation can be obtained unless the metal catalyst is employed. In addition, control experiments were performed under the above-mentioned reaction conditions but in the presence of $Cu(MeCOO)_2$, $Cd(MeCOO)_2{\cdot}2H_2O$, $Pd(MeCN)_2Cl_2$, $Co(NO_3)_2{\cdot}6H_2O$, or $Zn(NO_3)_2{\cdot}6H_2O$ as the source of catalytic centers. No appreciable conversion of CyH was observed.

2.10.2. Microwave-Assisted Solvent-Free Peroxidative Oxidation of 1-Phenylethanol with t-BuOOH. The solvent-free peroxidative oxidations of 1-phenylethanol were performed in a focused Anton Paar Monowave 300 reactor, using a 10 mL capacity reaction tube with a 13 mm internal diameter and equipped with a rotational system and an IR temperature detector. The alcohol (2.5 mmol), **M-dmpzc** (10 μmol, 0.4 mol % vs substrate), and an aqueous solution of *t*-BuOOH (5 mmol, 70%) were introduced to a cylindrical Pyrex tube, which was subsequently sealed. In the experiments performed in the presence of radical traps, either $CBrCl_3$ (2.5 mmol) or $NHPh_2$ (2.5 mmol) was added to the reaction mixture. The tube was then placed in the microwave reactor, and the system was left under stirring and under irradiation (20 W) at 80 or 120 °C for 0.5−3 h. After cooling to room temperature, 150 μL of benzaldehyde (as internal standard) and 2.5 mL of MeCN (to extract the substrate and the organic products from the reaction mixture) were added. The obtained mixture was stirred for 10 min; then a sample (1 μL) was taken from the organic phase and analyzed by GC using the internal standard method. The GC measurements were carried out using the FISONS Instruments gas chromatograph mentioned in section 2.10.1. The temperature of the injection was 240 °C. The column was initially maintained at 120 °C for 1 min, and then it was heated up to 200 °C with steps of 10 °C/min and held at this temperature for 1 min. The attribution of the observed GC peaks was carried out on the basis of chromatograms of pure 1-phenylethanol and acetophenone. Besides that, calibration curves were obtained with known concentrations of samples of pure products and standard and, in some cases, by GC−mass spectrometry analysis using a PerkinElmer Clarus 600 C instrument, equipped with a 30 m × 0.22 mm × 25 μm BPX5 (SGE) capillary column, and helium as the carrier gas. Control experiments were performed under the same reaction conditions but in the presence of $Cu(MeCOO)_2$, $Cd(MeCOO)_2{\cdot}2H_2O$, $Pd(MeCN)_2Cl_2$, $Co(NO_3)_2{\cdot}6H_2O$, or $Zn(NO_3)_2{\cdot}6H_2O$ as the source of catalytic centers. No appreciable conversion of the alcohol was observed. Moreover, blank experiments showed that no significant amount of products is obtained in the absence of any catalysts.

The catalyst recyclability was also tested; first, the used catalyst was separated from the reaction mixture by centrifugation, followed by filtration of the supernatant solution, washed with MeOH, and dried in oven overnight at 60 °C. A new reaction was performed by the addition of new portions (see the quantities specified above) of all reagents besides the recycled catalyst. After completion of the run, the products were analyzed as described above.

2.10.3. Nitroaldol (Henry) C−C Coupling of Nitroethane and Benzaldehyde. In a typical reaction, the **M-dmpzc** species (5 μmol) were added, under ambient conditions, to a capped glass vessel containing a mixture of nitroethane (286 μL, 4 mmol) and aldehyde (1 mmol). Then, either water or MeOH (2 mL) was added. The reaction mixture was kept under stirring for 24 h; then it was centrifuged to remove the solids. When water was employed as the solvent, the organic compounds were extracted from the reaction mixture with dichloromethane (2 × 2 mL). All of the extracted fractions were merged and dried with anhydrous sodium sulfate. Subsequent evaporation of the solvent yielded the crude product, which was dissolved in DMSO-d^6 and analyzed by ^{1}H NMR. The yield in β-nitroalkanol (relative to the aldehyde) was established by means of ^{1}H NMR spectroscopy,[23] using 1,2-dimethoxyethane as the internal standard. For the β-nitroalkanol products, the values of the vicinal coupling constants between the α-N−C−H and α-O−C−H protons (J = 7−9 or 3.2−4 Hz,[24] respectively) helped in identification of the syn or anti isomers. Control experiments were performed under the same reaction conditions but in the presence of $Cu(MeCOO)_2$, $Cd(MeCOO)_2{\cdot}2H_2O$, $Pd(MeCN)_2Cl_2$, $Co(NO_3)_2{\cdot}6H_2O$, or $Zn(NO_3)_2{\cdot}6H_2O$ as the source of catalytic centers. No appreciable formation of nitroaldol was observed. Moreover, blank experiments showed that no significant amount of products is obtained in the absence of any catalysts.

The catalyst recyclability was also tested; first, the used catalyst was separated from the reaction mixture by centrifugation, followed by filtration of the supernatant solution, washed with water and MeOH, and dried in air at room temperature. A new reaction was performed by the addition of new portions (see the quantities specified above) of all reagents besides the recycled catalyst. After completion of the run, the products were analyzed as described above.

2.10.4. Suzuki−Miyaura Cross-Coupling of Aryl Halides with Phenylboronic Acid. Potassium carbonate (0.15 mmol), bromoanisole (0.10 mmol), and phenylboronic acid (0.12 mmol) were mixed in a round-bottom flask, followed by the addition of **M-dmpzc** (in the range of 1×10^{-5}−1×10^{-3} mol) dissolved in ethanol (1 mL). The flask was placed in an oil bath preheated at 80 °C and allowed to set for 2−6 h. Then the reaction mixture was cooled to 25 °C and evaporated to dryness either under a stream of N_2 or in vacuo, followed by the addition of 1,2-dimethoxyethane (0.10 mmol), as the ^{1}H NMR standard, and extraction of the organic phase with $CDCl_3$ (4 × 0.20 mL). The extracted fractions were merged and analyzed by ^{1}H NMR spectroscopy. Assignment of the ^{1}H NMR signals was based on pure samples of substrates and product. ^{1}H NMR spectroscopy revealed that no coupling product was found, irrespective of the **M-dmpzc** compound employed: the signal due to the $-OCH_3$ protons of the substrate (ca. 3.77 ppm) was invariably the only signal observed,

DOI: 10.1021/acs.inorgchem.5b02997
Inorg. Chem. XXXX, XXX, XXX−XXX

whereas, if coupling would have been successful, the signal would have shifted approximately to 3.86 ppm.[25]

3. RESULTS AND DISCUSSION

3.1. Synthesis and Spectroscopic Characterization. The solvothermal reaction (DMF, 120−150 °C) of cadmium(II), zinc(II), and cobalt(II) salts with $dmpzc^{2-}$, obtained by in situ deprotonation of H_2dmpzc, enabled us to isolate polycrystalline powders formulated as **Cd-dmpzc**, **Zn-dmpzc·S**, and **Co-dmpzc·S**. In coupling cobalt(II) and zinc(II) to $dmpzc^{2-}$, we originally aimed to isolate CPs having the formula [M(dmpzc)] (M = Zn, Co), different from the already known $[M_4O(dmpzc)_3]$·Solv (M = Zn, Co) MAC frameworks showing the same pcu-a topology of MOF-5.[26] To this aim, different reaction paths were followed with respect to those that lead to $[M_4O(dmpzc)_3]$·Solv (M = Zn,[12b] Co[11]), adopting DMF instead of ethanol/water (zinc) or DMF/DMSO/MeOH (cobalt) as the solvent. In spite of this, **Zn-dmpzc·S** and **Co-dmpzc·S** were invariably obtained. For the sake of completeness, sections 2.6 and 2.7 report the synthetic paths optimized during this work. At least in the case of **Co-dmpzc·S**, a faster and higher-yield (65% vs 55%[11]) path was identified. The IR spectra of **Cd-dmpzc**, **Zn-dmpzc·S**, and **Co-dmpzc·S** (Figure 1a) reveal the absence of N−H stretching bands, as well as the presence of a carboxylate anion, water, and DMF.[27,28]

The room temperature reaction of bis(acetonitrile)-dichloropalladium(II) with H_2dmpzc in MeOH yielded **Pd-dmpzc** in the form of yellow polycrystalline powders. Unlike the other **M-dmpzc** derivatives, which are insoluble in water and in the most common solvents, **Pd-dmpzc** is soluble in DMF and DMSO. The presence of neutral H_2dmpzc spacers is confirmed by IR spectroscopy (Figures 1b vs S2).[29]

The interaction of copper(II) acetate with H_2dmpzc under reflux in distilled water afforded the violet compound **Cu-dmpzc** in the form of polycrystalline powders. It is worth noting that the synthetic procedure proposed here, allowing us to recover the compound in 1 day, is faster and grants a higher yield (55 vs 40%) than the 3-day previously reported path.[12d] The presence of a monoanionic ligand is confirmed by IR spectroscopy (Figure 1b).[30] To the best of our knowledge, besides determination of the crystal structure, a somehow incomplete (see section 3.3) investigation of the thermal behavior, and a study of the magnetic properties,[12d] no functional characterization has been ever carried out on **Cu-dmpzc**.

3.2. Crystal Structures. Within this section, the main structural features of the novel compounds **Cd-dmpzc** and **Pd-dmpzc** are described. For the sake of completeness, a brief description of the crystal structures of **Cu-dmpzc**, **Zn-dmpzc·S**, and **Co-dmpzc·S** is also provided. Overall, the four structural topologies described below demonstrate the coordination versatility of both H_2dmpzc and its mono- and dianionic forms.

Cd-dmpzc crystallizes in the monoclinic space group $P2_1/m$. The asymmetric unit is composed of two independent metal ions (Cd_1 and Cd_2, in the following), lying on a crystallographic mirror plane, two $dmpzc^{2-}$ spacers, lying on a mirror plane and on an inversion center, respectively, one DMF molecule and one water molecule, both lying in general positions. Cd_1 possesses a $CdNO_5$ octahedral stereochemistry defined by the oxygen atoms of two DMF molecules and the donor atoms of four $dmpzc^{2-}$ spacers (Figure 2a); more in detail, three ligands coordinate Cd_1 through one oxygen atom of their carboxylate groups, while the forth one is bound to Cd_1 through one nitrogen atom of the pyrazolate ring (Figure 2a). Cd_2 possesses a CdO_5 square-pyramidal coordination sphere defined by the oxygen atoms of two water molecules and three oxygen atoms of three ligands (one of which occupies the apical position, Figure 2a). Overall, the two independent ligands show an *exo*-tridentate coordination mode, involving the oxygen atoms of the carboxylate group and one nitrogen atom of the pyrazolate ring.[31] The mutual arrangement of nodes and spacers gives rise to a 3D architecture featuring rhombic channels parallel to the (101) crystallographic plane (Figure 2b). The coordinated DMF molecules protrude within the channels (Figure 2b), denying access to possible guest species. Indeed, no empty volume is present at room temperature.[32]

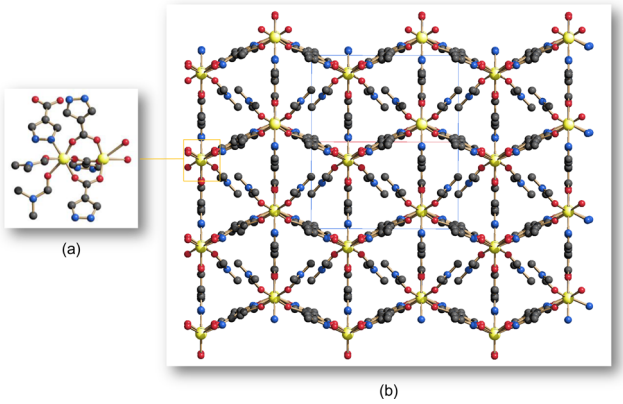

Figure 2. Representation of the crystal structure of **Cd-dmpzc**: (a) Coordination sphere of the two independent cadmium(II) ions. (b) Portion of the crystal packing viewed along the [101] direction. Color code: carbon, gray; cadmium, yellow; nitrogen, blue; oxygen, red. Hydrogen atoms have been omitted for clarity.

Pd-dmpzc crystallizes in the monoclinic space group $C2/c$. The asymmetric unit is composed of one metal ion, lying on an inversion center, one neutral H_2dmpzc ligand and one chloride ion, both situated in general positions. Each metal center shows a trans square-planar coordination sphere defined by two chloride ions and two nitrogen atoms of two ligands. H_2dmpzc acts as a nitrogen-donor monodentate ligand. The crystal structure is composed of monomeric units having the formula $[Pd(H_2dmpzc)_2Cl_2]$ (Figure 3a), connected by means of hydrogen-bonding interactions. Indeed, as was somehow expected, adjacent carboxylic groups are reciprocally hydrogen-bonded; this occurrence generates 1D zigzag chains running parallel to the crystallographic direction [100] (Figure 3b). Hydrogen bonds are present also along the crystallographic direction [001] between the chloride ions belonging to one chain and the N−H groups of nearby chains (Figure 3c). Overall, therefore, a 3D hybrid coordination/hydrogen-bonded network is formed. The latter possesses 1D ellipsoidal channels (Figure 3d) running parallel to the crystallographic direction [001]. Taking into account the van der Waals radii of the hydrogen atoms[33] of the methyl groups that protrude within the channels, the latter possess an aperture of ca. 4.6 Å, responsible for the presence of an empty volume, at room temperature, amounting to 38.4% of the unit cell volume.[32]

Cu-dmpzc crystallizes in the orthorhombic space group *Fdd*2. Each metal center shows a trans square-planar coordination sphere defined by two nitrogen atoms and two oxygen atoms belonging to four different ligands (Figure 4a). Each $Hdmpzc^-$ spacer acts as a *N,O-exo*-bidentate ligand and bridges adjacent metal centers 8.3262(3) Å apart, forming a 3D

DOI: 10.1021/acs.inorgchem.5b02997
Inorg. Chem. XXXX, XXX, XXX−XXX

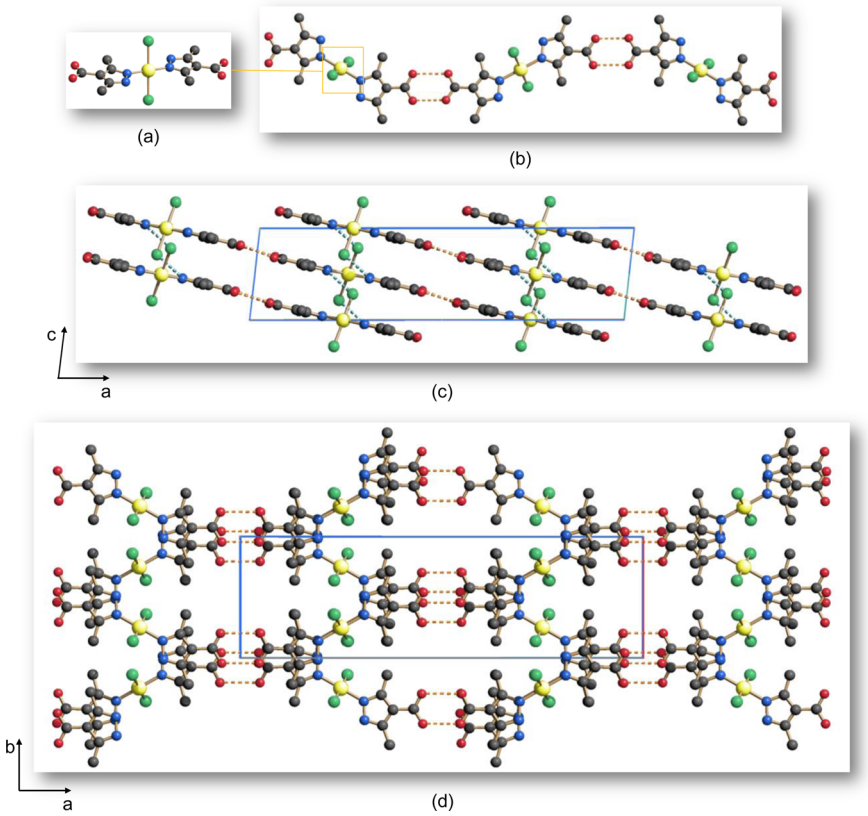

Figure 3. Representation of the crystal structure of **Pd-dmpzc**: (a) Coordination sphere of palladium(II). (b) Portion of the 1D chain generated by hydrogen-bonding interactions (orange dashed lines) involving adjacent carboxylic groups. (c) Portion of the crystal packing viewed along the crystallographic direction [010] (horizontal axis, *a*; vertical axis, *c*): the Cl···H−N hydrogen bonds have been depicted with cyan dashed lines. (d) Portion of the crystal packing viewed in perspective along the crystallographic direction [001] (horizontal axis, *a*; vertical axis, *b*). Color code: carbon, gray; chlorine, green; nitrogen, blue; oxygen, red; palladium, yellow. Hydrogen atoms have been omitted for clarity.

diamondoid network (Figure 4c), in which square meshes parallel to the (110) plane are present (Figure 4b). The methyl groups of the ligands protrude within the meshes, so that no empty volume is present.[32] The framework is further strengthened by the presence of hydrogen bonds running parallel to the crystallographic direction [001] and involving the uncoordinated oxygen atom of one ligand and the N−H group of an adjacent pyrazole ring.

The two porous MAC frameworks **Zn-dmpzc·S**[12b] and **Co-dmpzc·S**[11] are isostructural and possess the cubic pcu-a topology of MOF-5. Hence, they feature M_4O nodes (Figure 5a), connected to six nearby ones by *N,N′,O,O′-exo*-tetradentate spacers within a 3D porous framework (Figure 5b). Rather narrow windows lead to ca. 6 Å wide cavities accounting for an empty volume amounting to ca. 45% at room temperature.[32]

3.3. Thermal Behavior. To evaluate the thermal behavior of the five MAC compounds, TGA (Figure 6), performed under a N_2 flow, was coupled with VT-PXRD, carried out in air.

Cd-dmpzc is stable up to 250 °C both under N_2 and in air (Figures 6 and 7a): the 26% mass loss observed in the temperature range of 250−350 °C (Figure 6) corresponds to the loss of one DMF molecule and one water molecule *per* formula unit (theoretical loss: 26.6%). The loss of solvent molecules at such a high temperature, well above their boiling points, suggests that they are bound to the metal centers through strong coordinative bonds. Already at 350 °C, immediately after the complete loss of solvent, decomposition takes place. VT-PXRD substantiates this evidence and provides further information. In the temperature range of 250−350 °C[21] (Figure 7a, light-green region), solvent loss is accompanied by the disappearance of **Cd-dmpzc**, concomitant with the appearance and growth of a new low-crystallinity phase. **Cd-dmpzc** definitely disappears at 370 °C: a PXRD acquisition, carried out at 370 °C up to $2\theta = 60°$, enabled us to detect the presence of cadmium(II) oxide. The Le Bail parametric treatment of the PXRD data of **Cd-dmpzc** in the range of 30−290 °C highlights a very modest variation of the unit cell parameters[34] (Figure 7b), resulting into a volumetric thermal expansion of 1.1%. Finally, the material is recovered intact after five heating−cooling cycles in the temperature range of 30−150 °C (Figure 7c), thus surviving to consecutive thermal stresses, an encouraging aspect in view of possible practical applications.

Compound **Pd-dmpzc** is stable up to 300 °C under N_2 (Figure 6) and in air: VT-PXRD shows that it starts to lose crystallinity around 300 °C[21] (Figure S3a) and does not undergo phase transitions prior to decomposition. The Le Bail parametric treatment of the PXRD data in the temperature range of 30−290 °C highlights (Figure S3b) an overall volumetric thermal expansion of 3.7%. In particular,[35] the expansion is moderate along the *ab* plane; definitely more significant is the increment of the crystallographic axis *c*, along which the N−H···Cl hydrogen bonds are at work (Figure 3c). In light of this, we suggest that heating might favor a weakening of the N−H···Cl nonbonding interactions. Finally, **Pd-dmpzc** is

DOI: 10.1021/acs.inorgchem.5b02997
Inorg. Chem. XXXX, XXX, XXX−XXX

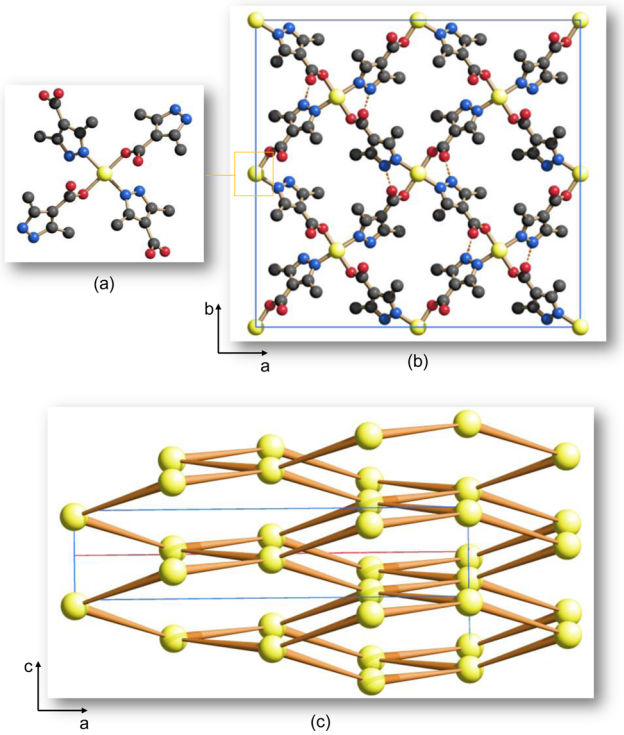

Figure 4. Representation of the crystal structure of **Cu-dmpzc**: (a) Coordination sphere of the copper(II) ion. (b) Portion of the crystal packing viewed along the crystallographic direction [001] (horizontal axis, *a*; vertical axis, *b*). N–H···O hydrogen-bonding interactions have been represented with orange dashed lines. (c) Portion of the underlying diamondoid network viewed, in perspective, along the [010] direction (horizontal axis, *a*; vertical axis, *c*). Color code: carbon, gray; copper, yellow; nitrogen, blue; oxygen, red. Hydrogen atoms have been omitted for clarity.

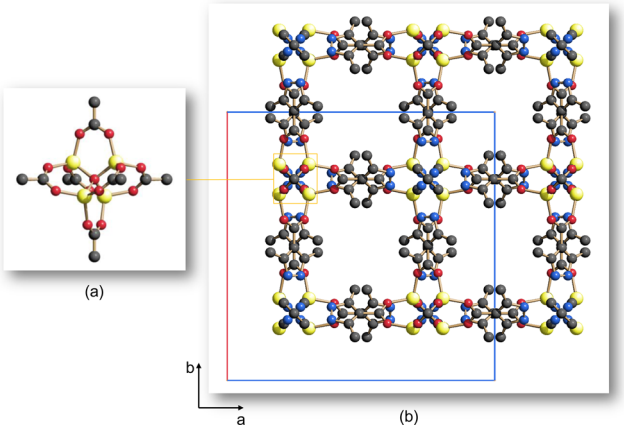

Figure 5. Representation of the crystal structure of **Zn-dmpzc·S**: (a) The node. (b) Portion of the crystal packing viewed along the crystallographic direction [001] (horizontal axis, *a*; vertical axis, *b*). Color code: carbon, gray; nitrogen, blue; oxygen, red; zinc, yellow. Hydrogen atoms and solvent molecules have been omitted for clarity.

recovered intact after five heating–cooling cycles in the temperature range of 30–150 °C (Figure S3c).

The thermal behavior of **Cu-dmpzc** was previously investigated by coupling TGA and VT-PXRD.[12d] The authors ended the VT-PXRD acquisition at 240 °C and, consequently, claimed that the material, in air, preserves its structural integrity

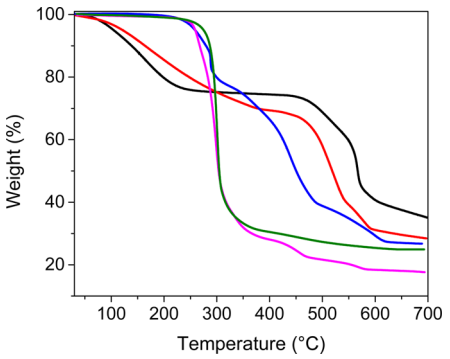

Figure 6. TGA traces of **Cd-dmpzc** (blue), **Pd-dmpzc** (green), **Cu-dmpzc** (fuchsia), **Zn-dmpzc·S** (black), and **Co-dmpzc·S** (red).

up to that temperature. The TGA and VT-PXRD experiments carried out in the present work allowed us to complete this information. **Cu-dmpzc** is stable up to 275 °C (TGA evidence), the temperature at which the material starts to lose crystallinity (VT-PXRD evidence; Figure S4a). VT-PXRD also demonstrates that no phase transitions take place up to decomposition: the material is therefore slightly more stable than that envisaged by Chen and co-workers.[12d] The Le Bail parametric treatment of the data acquired in the temperature range of 30–270 °C highlights a modest variation of the unit cell parameters[36] (Figure S4b), with an overall volumetric thermal expansion of 1.1%. Finally, **Cu-dmpzc** is recovered intact after five heating–cooling cycles in the temperature range of 30–150 °C (Figure S4c).

The TGA traces of **Zn-dmpzc·S** and **Co-dmpzc·S** (Figure 6) show progressive weight losses of 25% (in the range of 30–250 °C) and 31% (in the range of 30–450 °C), respectively, corresponding to the loss of all of the clathrated solvent molecules (theoretical losses 25.4 and 31.7%, respectively). In both cases, at 450 °C, a slow decomposition begins. VT-PXRD[12b] not only highlights that **Zn-dmpzc·S** preserves its structural features and high crystallinity up to decomposition but also demonstrates the rigidity of the framework, undergoing a slight unit cell volume contraction amounting to −0.5% upon heating, which could be attributed to the release of the guest solvent molecules. The behavior of **Co-dmpzc·S** is not monotonic (Figure S6a); its framework is even more rigid than that of the zinc(II) counterpart: more in detail, the −0.15% contraction of the unit cell volume in the temperature range of 30–190 °C can be attributed to solvent molecules release from the 1D channels, followed by a slight thermal expansion of 0.1% in the temperature range of 190–330 °C. Finally, **Zn-dmpzc·S** and **Co-dmpzc·S** survive along five heating–cooling cycles in the temperature range of 30–150 °C (Figures S5 and S6b).

3.4. Catalytic Applications. *3.4.1. Oxidation of Alkanes and Alcohols with t-BuOOH.* After thermal activation of **Zn-dmpzc·S** and **Co-dmpzc·S**, all of the **M-dmpzc** materials were tested as catalysts in the oxidation of CyH with *tert*-butyl hydroperoxide (*t*-BuOOH; aqueous, 70%) in MeCN under relatively mild conditions (in air, at 50 °C and ambient pressure; Scheme 2, reaction a). The oxidation of CyH to cyclohexyl hydroperoxide (CyOOH; primary product), CyOH, and CyO, which are typically the final products, was monitored by GC after treatment of the aliquot extracted from the reaction mixture with PPh_3 (to reduce CyOOH to CyOH). **Cu-dmpzc** and **Co-dmpzc** revealed the highest catalytic activity

DOI: 10.1021/acs.inorgchem.5b02997
Inorg. Chem. XXXX, XXX, XXX–XXX

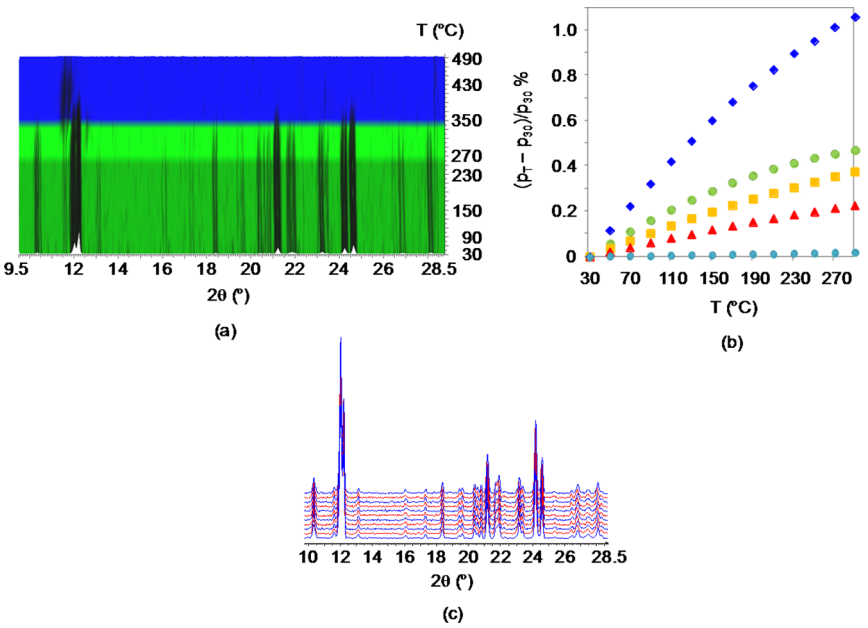

Figure 7. (a) Plot of the PXRD patterns measured on **Cd-dmpzc** as a function of the temperature heating in air, with steps of 20 °C, from 30 °C up to decomposition: (green region) as-synthesized phase; (light-green region) coexistence of as-synthesized and novel phase; (blue region) novel phase. (b) Percentage variation of the unit cell parameters (p_T) of **Cd-dmpzc** as a function of the temperature. At each temperature, the actual values (p_T) have been normalized with respect to those at 30 °C (p_{30}). *a*, green circles; *b*, orange squares; *c*, red triangles; *β*, cyan circles; *V*, blue rhombi. (c) Plot of the PXRD patterns measured on **Cd-dmpzc** along five heating−cooling cycles in the temperature range of 30−150 °C: heating step, red; cooling step, blue.

Scheme 2. Peroxidative Oxidations, with *tert*-Butyl Hydroperoxide, of (a) CyH and (b) 1-Phenylethanol, Performed by Using the M-dmpzc (M = Co, Cu, Zn, Pd, Cd) Compounds as Catalysts

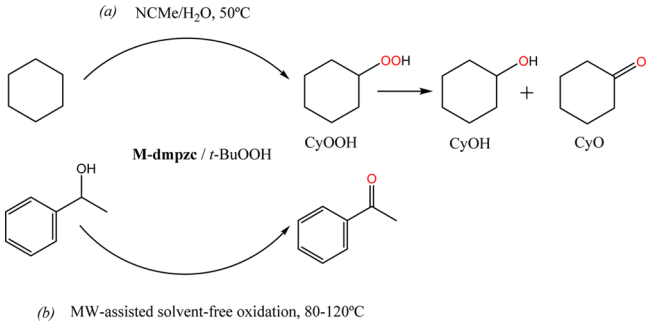

under the essayed experimental conditions: while **Cu-dmpzc** exhibits an average activity (yields up to 12%), the latter is somehow less efficient (yields up to 8%). **Cd-dmpzc**, **Pd-dmpzc**, and **Zn-dmpzc** are almost inactive (yields up to 1%). Because **Zn-dmpzc** and **Co-dmpzc** are isostructural but show different activities, we suggest that the nature of the metal ion reasonably plays a prominent role in this catalytic reaction.

In the applied conditions, the recovery and isolation of the catalysts from the reaction mixture after the oxidation reaction were not possible, thus hampering recyclability tests.

The beneficial effect of an acid cocatalyst in the oxidation of alkanes has been observed for other catalytic systems.[37] The overall yields in oxygenated products (CyOH and CyO), obtained in the absence and in the presence of TFA, are reported in Table 1 and Figures 8 and 9. **Cu-dmpzc** catalyzes the oxidation reaction in the absence of any added acid with an overall yield, reached after ca. 30 min, amounting approximately to 3% (Table 1, entry 1). An increase of the reaction time enhances the overall yield up to ca. 9% after 12 h (Table 1, entry 7). The activity exhibited by **Cu-dmpzc** in the absence of TFA after 6 h of reaction (7.4% total yield, Table 1, entry 5) is higher than that shown, e.g., by $[Cu(OTf)_2(Py_2S_2)]$ (Py_2S_2 = 1,6-bis(2′-pyridyl)-2,5-dithiahexane; 4.3% total yield after 6 h)[38] or by $NH_4[Cu_3\text{-}(\mu^3\text{-}OH)(\mu^3\text{-}4\text{-carboxypyrazolato})_3]$ (yielding 4% CyO as a single product at 70 °C after 24 h).[12a] However, comparable results were obtained in the presence of complexes bearing azathia macrocycles, e.g., $[Cu(OTf)_2(L^3)]$ (L^3 = mixed 14-membered N_2S_2 azathia macrocycle) or $[Cu(OTf)(L^4)(H_2O)](OTf)$ (L^4 = nine-membered NS_2 macrocyclic ligand with a 2-methylpyridyl pendant arm) (overall yield of ca. 8% after 6 h).[39] The presence of TFA improves the catalytic performance of **Cu-dmpzc**: the total yield achieves a maximum value of ca. 12% after 9 h (Table 1, entry 14).

The formation of CyOOH (typical primary product in radical-type CyH oxidations),[36,40] along with the complete suppression of the catalytic activity upon the introduction of a radical trap (Ph_2NH or $CBrCl_3$) to the reaction mixture (entries 37 and 38 in Table 1), supports a free-radical reaction mechanism. The reaction is possibly initiated by metal-catalyzed decomposition of the peroxide, leading to the radicals *t*-BuOO$^\bullet$ and *t*-BuO$^\bullet$, which form the cycloalkyl radical Cy$^\bullet$ upon hydrogen abstraction from CyH. Cy$^\bullet$ reacts with oxygen, leading to CyOO$^\bullet$. CyOOH can be formed, e.g., upon hydrogen abstraction from ROOH by CyOO$^\bullet$. Metal-assisted decomposition of CyOOH to CyO$^\bullet$ would then lead to CyOH and CyO products.

The **M-dmpzc** MAC compounds were tested as catalysts also in the oxidation of 1-phenylethanol to acetophenone (Scheme 2, reaction b) following a procedure recently developed by us,[41] employing *t*-BuOOH (aqueous, 70%) as the oxidizing agent, under typical conditions of 80−120 °C, microwave irradiation

DOI: 10.1021/acs.inorgchem.5b02997
Inorg. Chem. XXXX, XXX, XXX−XXX

Table 1. Total Yield (CyOH and CyO), as a Function of Time, in the Oxidation of CyH by *t*-BuOOH (Aqueous, 70%) Catalyzed by M-dmpzc at 50 °C in CH_3CN[a]

				yield (%)[b]		
entry	catalyst	cocatalyst	reaction time (h)	CyOH	CyO	total
1	**Cu-dmpzc**		0.5	1.7	1.2	2.9
2			1	2.2	1.4	3.6
3			3	2.7	1.7	5.4
5			6	4.9	2.4	7.3
6			9	5.5	2.7	8.2
7			12	5.8	3.1	8.9
9		TFA	0.5	2.9	1.9	4.8
10		TFA	1	3.9	2.2	6.1
11		TFA	3	6.2	2.7	8.9
12		TFA	6	7.6	3.6	11.2
13		TFA	9	8.2	3.7	11.9
14		TFA	12	8.1	4.0	12.1
15	**Co-dmpzc**		0.5	0.3	0.4	0.7
16			1	1.0	0.6	1.6
17			3	1.3	1.2	2.5
18			6	2.5	1.2	3.7
19			9	3.0	1.9	4.9
20			12	3.4	2.1	5.5
21		TFA	0.5	2.2	1.1	3.1
22		TFA	1	2.8	1.2	4.0
23		TFA	3	3.2	2.0	5.2
24		TFA	6	3.9	2.9	6.8
25		TFA	9	4.1	3.1	7.2
26		TFA	12	4.5	3.8	8.3
27	**Zn-dmpzc**	TFA	9	0.2	0.2	0.4
28	**Pd-dmpzc**	TFA	9	0.5	0.7	1.2
29	**Cd-dmpzc**	TFA	9	0.4	0.4	0.8
30			9	0.0	0.0	0.0
31		TFA	9	0.0	0.0	0.0
32	$Cu(MeCOO)_2$	TFA	9	1.9	1.3	3.2
33	$Co(NO_3)_2{\cdot}6H_2O$	TFA	9	1.8	1.1	2.9
34	$Zn(NO_3)_2{\cdot}6H_2O$	TFA	9	0.0	0.0	0.0
35	$Cd(MeCOO)_2{\cdot}2H_2O$	TFA	9	0.2	0.1	0.3
36	$Pd(MeCN)_2Cl_2$	TFA	9	0.2	0.0	0.2
37[c]	**Cu-dmpzc**	TFA	9	0.0	0.0	0.0
38[d]		TFA	9	0.0	0.0	0.0

[a]Reaction conditions: CyH (0.46 M), **M-dmpzc** (2.5 μmol), TFA (5×10^{-3} M), *t*-BuOOH (70% in H_2O, 0.56 M), in CH_3CN (total volume of the reaction solution, 5 mL), 50 °C. [b]Moles of products (CyOH + CyO) *per* 100 mol of CyH, as determined by GC after treatment with PPh_3. [c]In the presence of Ph_2NH (2.3 mmol). [d]In the presence of $CBrCl_3$ (2.3 mmol).

(20 W), for a 0.5−3 h reaction time and in the absence of any added solvent. All **M-dmpzc** compounds showed catalytic activity in this oxidation reaction (Table 2): **Cu-dmpzc**, **Co-dmpzc**, and **Pd-dmpzc** exhibited the best catalytic performances in the essayed experimental conditions. Although **Zn-dmpzc** and **Co-dmpzc** are isostructural, the former is much less active (38% yield; Table 2, entry 15) than the latter (64% yield; Table 2, entry 11). Once again, and given also the exceptional performance of the copper derivative (see below), the metal ion reasonably plays a key role in such a catalytic reaction.

Using **M-dmpzc**, acetophenone is the only oxidation product obtained in the adopted experimental conditions. The high

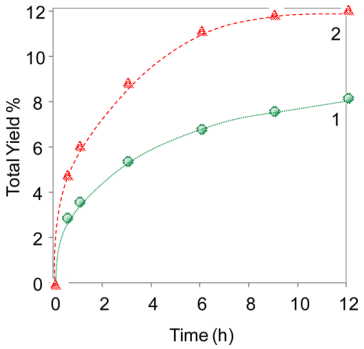

Figure 8. Total yield (CyOH and CyO), as a function of time, in the oxidation of CyH (0.46 M) by *t*-BuOOH (aqueous, 70%, 0.56 M) catalyzed by **Cu-dmpzc** (5×10^{-4} M) in the absence of any additive (curve 1) or in the presence of TFA (1:10 catalyst/acid molar ratio) (curve 2) at 50 °C in CH_3CN.

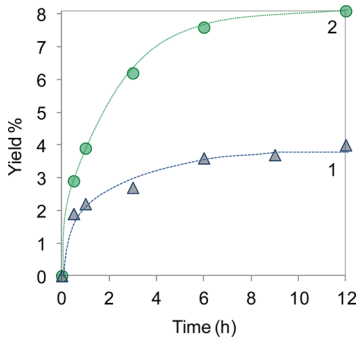

Figure 9. Accumulation of oxygenated products (CyOH, curve 1; CyO, curve 2) as a function of time in the oxidation of CyH (0.46 M) with *t*-BuOOH (aqueous, 70%, 0.56 M) catalyzed by **Cu-dmpzc** (5×10^{-4} M) in MeCN (total volume of the reaction solution, 5 mL) at 50 °C. The concentration of the products was measured after their reduction with PPh_3.

selectivity observed (typically >98%) was confirmed, in all cases, by mass balance.

Under typical reaction conditions (80 °C and 0.5 h reaction time), yields of 40% and 25% were obtained with **Cu-dmpzc** and **Co-dmpzc**, respectively, for a catalyst/substrate molar ratio of 0.4% and in the absence of any additive (Table 2, entries 1 and 7). For a longer reaction time (3 h), the oxidation of 1-phenylethanol by *t*-BuOOH led to 64 and 40% of acetophenone (Table 2, entries 3 and 9) for **Cu-dmpzc** and **Co-dmpzc**, respectively.

The hypothesis of significant leaching under the tested conditions was verified in the case of **Cu-dmpzc**: no acetophenone was formed in a typical assay performed with the reaction solution recovered after filtration from the first run (Table 2, entry 7) and taken to dryness, to which new portions of all reagents except the catalyst were added. On the other hand, the catalyst recovered by filtration from the first run was tested in a subsequent reaction by the addition of fresh reagents: only 62% yield of acetophenone was obtained (Table 2, entry 29). A PXRD analysis enabled us to assess that, after the first run, the catalyst recovered is slightly impure and has lost crystallinity with respect to a fresh sample.

Temperature has an important accelerating effect on the conversion of 1-phenylethanol: at 120 °C, a yield of 97% or 64% was obtained after 30 min reaction in the presence of **Cu-dmpzc** or **Co-dmpzc**, respectively (Table 2, entries 4 and 11).

DOI: 10.1021/acs.inorgchem.5b02997
Inorg. Chem. XXXX, XXX, XXX−XXX

Table 2. Selected Results for the Microwave-Assisted Oxidation of 1-Phenylethanol by *t*-BuOOH with M-dmpzc as the Catalyst[a]

entry	catalyst	reaction time (h)	temperature (°C)	additive (μmol)	yield[b] (%)	TON[c] (TOF)[d]
1	**Cu-dmpzc**	0.5	80		40	100 (200)
2		1	80		47	118 (118)
3		3	80		64	160 (53)
4		0.5	120		97	243 (485)
5		0.5	80	TEMPO (30)	43	108 (215)
6		3	80	TEMPO (30)	71	178 (59)
7		0.5	120	TEMPO (30)	99	248 (495)
8	**Co-dmpzc**	0.5	80		25	63 (125)
9		1	80		31	78 (78)
10		3	80		40	100 (33)
11		0.5	120		64	160 (320)
12		0.5	80	TEMPO (30)	27	68 (135)
13		0.5	120	TEMPO (30)	62	155 (310)
14	**Zn-dmpzc**	0.5	80		9	23 (46)
15		0.5	120		38	95 (190)
16	**Pd-dmpzc**	0.5	80		18	45 (90)
17		0.5	120		64	160 (320)
18	**Cd-dmpzc**	0.5	80		5	13 (26)
19		0.5	120		16	40 (80)
20		0.5	120		0	
21				TEMPO (30)	0	
22	$Cu(MeCOO)_2$	0.5	120	TEMPO (30)	5	13 (26)
23	$Co(NO_3)_2{\cdot}6H_2O$				4	10 (20)
24	$Zn(NO_3)_2{\cdot}6H_2O$				4	11 (22)
25	$Cd(MeCOO)_2{\cdot}2H_2O$				2	5 (9)
26	$Pd(MeCN)_2Cl_2$				2	6 (13)
27	**Cu-dmpzc**	0.5	120	Ph_2NH (2500)	0	0
28				$CBrCl_3$ (2500)	0	0
29	recovered from entry 7	0.5	120	TEMPO (30)	62	155 (310)

[a]Reaction conditions (unless stated otherwise): 2.5 mmol of substrate, 10 μmol of catalyst (0.4 mol % vs substrate), 5 mmol of *t*-BuOOH (aqueous, 70%), 80−120 °C, microwave irradiation (20 W). [b]Molar yield (%) based on substrate, i.e., moles of product *per* 100 mol of substrate as determined by GC. [c]Turnover number = number of moles of product *per* mole of metal catalyst. [d]Turnover frequency = turnover number *per* hour.

The presence of 2,2,6,6-tetramethylpiperydil-1-oxyl (TEMPO), known as an efficient promoter in the aerobic oxidation of alcohols,[42] did not significantly affect the yield: namely, in the presence of **Cu-dmpzc**, TEMPO enabled us to obtain slightly higher yields (43 or 99%, in the presence of TEMPO at 80 or 120 °C, respectively, vs 40 or 97%, in the absence of TEMPO at 80 or 120 °C, respectively; see Table 2, entries 1, 4, 5, and 7), whereas in the system catalyzed by **Co-dmpzc**, a slight decrease was observed [62% in the presence of TEMPO (Table 2, entry 13) vs 64% in the absence of TEMPO (Table 2, entry 11)]. This inhibiting effect is not surprising because it was already observed for other catalytic systems, namely, in the solvent-free microwave-assisted oxidation of 1-phenylethanol in the presence of the Schiff base copper(II) complexes $[Cu_4(\mu_4\text{-}O)(\mu_2\text{-}L^1)Cl_4]$ and $[Cu_4(\mu_4\text{-}O)(L^2)_2Cl_4]$, derived from 2,6-diformyl-4-methylphenol (DFF) and 1,3-bis(aminopropyl)tetramethyldisiloxane and from DFF and trimethylsilyl *p*-aminobenzoate, respectively.[37c]

In the tested conditions, on the basis of suppression of the catalytic activity obtained by the introduction of a radical trap (Ph_2NH or $CBrCl_3$) to the reaction mixture (Table 2, entries 27 and 28), a radical mechanism is proposed for the oxidation of 1-phenylethanol by *t*-BuOOH, similar to those proposed in other cases.[3b,36,40a,41] The mechanism might involve the microwave-assisted generation of *t*-BuOO$^\bullet$ and *t*-BuO$^\bullet$ radicals,[43] which behave as hydrogen-atom abstractors from the alcohol.

3.4.2. Nitroaldol (Henry) C−C Coupling of Nitroethane with Aldehydes. The catalytic activity of **M-dmpzc** was tested at room temperature, in MeOH or water, in the nitroaldol reaction between an aromatic aldehyde and nitroethane to yield the corresponding β-nitroalkanol (Scheme 3).

Scheme 3. Nitroaldol (Henry) C−C Coupling Reaction between an Aromatic Aldehyde (R = H, NO_2, Cl, Me, MeO) and Nitroethane, Performed by Adopting the M-dmpzc (M = Co, Cu, Zn, Pd, Cd) Derivatives as Catalysts

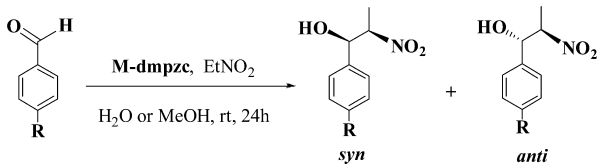

According to ^{1}H NMR spectroscopy, the products of the Henry reaction catalyzed by **M-dmpzc** are a mixture of the corresponding β-nitroalkanol diastereoisomers (syn and anti forms, with a general predominance of the former; Table 3). Stereochemical control of the newly generated carbon centers is rather difficult, in particular because of easy epimerization of the nitro substituent on the carbon chain.[44]

Zn-dmpzc and **Cd-dmpzc** exhibit the highest catalytic activities, leading to almost quantitative yields (e.g., for 4-nitrobenzaldehyde, entries 13 and 33; Table 3) in water at

DOI: 10.1021/acs.inorgchem.5b02997
Inorg. Chem. XXXX, XXX, XXX−XXX

Table 3. Selected Results for the Henry C−C Coupling Reaction Catalyzed by M-dmpzc[a]

entry	catalyst	substrate	solvent	yield (%)[b]	selectivity anti:syn[b]
1	**Cu-dmpzc**	4-nitrobenzaldehyde	H_2O	78	32:68
2			MeOH	73	27:73
3		benzaldehyde	H_2O	75	36:64
4			MeOH	75	39:61
5		4-methoxybenzaldehyde	H_2O	69	29:71
6			MeOH	60	42:58
7	**Co-dmpzc**	4-nitrobenzaldehyde	H_2O	81	26:74
8			MeOH	79	28:72
9		benzaldehyde	H_2O	74	21:79
10			MeOH	71	33:67
11		4-methoxybenzaldehyde	H_2O	52	31:69
12			MeOH	51	37:63
13	**Zn-dmpzc**	4-nitrobenzaldehyde	H_2O	98	24:76
14			MeOH	93	29:71
15		4-chlorobenzaldehyde	H_2O	88	33:67
16			MeOH	87	36:64
17		benzaldehyde	H_2O	86	27:73
18			MeOH	86	39:61
19		4-methylbenzaldehyde	H_2O	78	40:60
20			MeOH	75	38:62
21		4-methoxybenzaldehyde	H_2O	67	32:68
22			MeOH	63	48:52
23	**Pd-dmpzc**	4-nitrobenzaldehyde	H_2O	62	37:63
24			MeOH	61	39:61
25		4-chlorobenzaldehyde	H_2O	52	43:57
26			MeOH	45	48:52
27		benzaldehyde	H_2O	41	41:59
28			MeOH	48	31:69
29		4-methylbenzaldehyde	H_2O	35	32:68
30			MeOH	43	36:64
31		4-methoxybenzaldehyde	H_2O	33	42:58
32			MeOH	30	45:55
33	**Cd-dmpzc**	4-nitrobenzaldehyde	H_2O	97	27:73
34			MeOH	95	30:70
35		4-chlorobenzaldehyde	H_2O	89	28:72
36			MeOH	87	39:61
37		benzaldehyde	H_2O	79	40:60
38			MeOH	86	49:51
39		4-methylbenzaldehyde	H_2O	77	31:69
40			MeOH	73	31:69
41		4-methoxybenzaldehyde	H_2O	69	37:63
42			MeOH	68	42:58
43	$Cu(MeCOO)_2$	4-nitrobenzaldehyde	H_2O	9	29:71
44	$Co(NO_3)_2{\cdot}6H_2O$			11	32:68
45	$Zn(NO_3)_2{\cdot}6H_2O$			13	28:72
46	$Cd(MeCOO)_2{\cdot}2H_2O$			10	30:70
47	$Pd(MeCN)_2Cl_2$			6	39:61
48		4-nitrobenzaldehyde	MeOH	0	
49			H_2O	0	
50	recovered from entry 13	4-nitrobenzaldehyde	H_2O	50	32:68

[a]Reaction conditions: 5 μmol of catalyst, MeOH or water (2 mL), nitroethane (4 mmol), and aldehyde (1 mmol), in air, at room temperature, 24 h. [b]Determined by ^{1}H NMR analysis (see the Experimental Section).

room temperature, with an appreciable diastereoselectivity toward the syn isomer (anti/syn molar ratios of 24:76 and 27:73, respectively; Table 3). It is worth noting that water was a more convenient solvent than MeOH for this C−C coupling reaction, allowing higher yields and better stereochemical control (Table 3). For the other essayed **M-dmpzc** compounds, the reactivity order is Co > Cu > Pd (Table 3). Again, considering the existing structural similarities among the zinc(II) and cobalt(II) derivatives, the metal center must display a crucial role on the catalytic activity of these compounds. No significant Henry reaction between the tested aldehydes and nitroethane was observed in the absence of **M-dmpzc** but in the presence of $Cu(MeCOO)_2$, $Co(NO_3)_2.6H_2O$, $Zn(NO_3)_2{\cdot}6H_2O$, $Cd(MeCOO)_2{\cdot}2H_2O$, or

DOI: 10.1021/acs.inorgchem.5b02997
Inorg. Chem. XXXX, XXX, XXX−XXX

$Pd(MeCN)_2Cl_2$ as the source of catalytic centers (Table 3, entries 43−47).

The hypothesis of significant leaching under the tested conditions was verified for **Zn-dmpzc**: no nitroalkanol was formed in a typical assay performed with the solution recovered from a first run (Table 3, entry 13) after filtration and taken to dryness, to which new portions of all reagents except the catalyst were added. The catalyst recovered by filtration from the first run was tested in a subsequent reaction by the addition of fresh reagents: only 50% of the nitroalkanol mixture was obtained (Table 3, entry 50). Also in this case, a PXRD analysis allowed us to assess that, after the first run, the catalyst recovered is slightly impure and has lost crystallinity with respect to a fresh sample. The nature of substrates greatly influences the yield and selectivity. Benzaldehydes bearing the electron-withdrawing $-NO_2$ substituent at the aromatic ring (Table 3, entries 13, 14, 23, 24, 33, and 34) exhibit considerably higher reactivity compared to that of the benzaldehyde having, e.g., the electron-donor $-CH_3$ group in the same position (Table 3, entries 19, 20, 29, 30, 39, and 40). This evidence may be related to the decreasing electrophilicity of the aldehyde along the series. According to recent publications,[45] the reaction mechanism is expected to involve metal-assisted (upon coordination) deprotonation of the methylene group of nitroethane (to give a nitronate species), followed by activation of the aldehyde for its electrophilic attack (with C−C coupling) toward the nitronate. Hence, the **M-dmpzc** materials tested in the present work appear to be able to act as Lewis acids for the above-quoted activations.

As a preliminary study, we attempted to correlate the average crystal size, retrieved by PXRD, and catalytic activity for the two oxidation reactions and the Henry C−C coupling reaction tested. An inverse linear correlation seems to exist for the Henry C−C coupling reaction (Figure S7), suggesting that the exposed surface of the catalyst plays a nonnegligible role. On the other hand, the average crystal size seems to have a marginal role in the CyH oxidation reaction (Figure S7). Yet, a word of caution is necessary at this point: the model we adopted to estimate the average crystal size (Scherrer's law) assumes, as a first approximation, a spherical morphology for the crystallites. Hence, for a more complete picture and a more sensible correlation, the crystallite morphology should also be derived and taken into consideration, which is out of the scope of this work.

3.4.3. Suzuki−Miyaura Cross-Coupling of Bromoanisole with Phenylboronic Acid. Although no significant activity was expected for the **M-dmpzc** materials but the palladium(II) derivative, all of them were tested as catalysts for the Suzuki−Miyaura cross-coupling reaction of bromoanisole with phenylboronic acid, in the presence of a base, at 80 °C (Scheme 4), a renowned C−C coupling catalyzed by palladium(II) *monomeric* complexes.[25] Despite the different loads of **M-dmpzc** and reaction times adopted, less than 5% coupling product was detected in the essayed conditions (see section 2.10.4).

Scheme 4. Suzuki−Miyaura C−C Cross-Coupling Reaction of Bromoanisole with Phenylboronic Acid, Carried Out by Employing the M-dmpzc (M = Co, Cu, Zn, Pd, Cd) Compounds as Catalysts

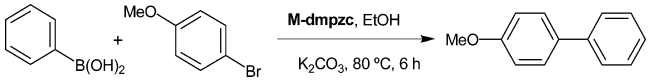

Possibly, the coordination/hydrogen-bonded polymeric network somehow hampers the catalytic activity of our palladium(II) derivative.

4. CONCLUSIONS

Five metal/azolate carboxylate compounds, built up with the H_2dmpzc ligand, have been synthesized and tested as catalysts in oxidation or Henry C−C coupling reactions. **Cu-dmpzc** and **Co-dmpzc** are the most active catalysts in both the partial oxidation of CyH by *tert*-butyl hydroperoxide in MeCN and the solvent-free microwave-assisted oxidation of 1-phenylethanol to acetophenone. It is worth noting the remarkable activity exhibited by **Cu-dmpzc** in the latter system (yields up to 99% at 120 °C after only 0.5 h). On the other hand, **Zn-dmpzc** is the most active **M-dmpzc** derivative in the Henry C−C coupling reaction of aromatic aldehydes with nitroethane, showing considerable diastereoselectivity toward the *syn*-nitroalkanol isomer. On the basis of the present results, the design of these materials seems to be worth of further development toward more effective (in particular, recyclable) catalysts, a topic that will be addressed in our future studies.

■ ASSOCIATED CONTENT

Ⓢ Supporting Information

The Supporting Information is available free of charge on the ACS Publications website at DOI: 10.1021/acs.inorgchem.5b02997.

X-ray crystallographic data in CIF format (CIF)
Crystal X-ray analysis, IR spectroscopy, thermal behavior, and catalytic activity (PDF)

■ AUTHOR INFORMATION

Corresponding Authors

*E-mail: lmartins@deq.isel.ipl.pt.
*E-mail: pombeiro@tecnico.ulisboa.pt.
*E-mail: simona.galli@uninsubria.it.
*E-mail: claudio.pettinari@unicam.it.

Notes

The authors declare no competing financial interest.

■ ACKNOWLEDGMENTS

The University of Insubria is acknowledged for partial funding. S.G. acknowledges the precious experimental help of Maria Giacchero. This work was partly supported by the PRIN-2010-BNZ3F2 Research Project DESCARTES, funded by the Italian Ministry of the University and Research and by the University of Camerino. Financial support from the Fundação para a Ciência e a Tecnologia, Portugal (Projects PTDC/QEQ-ERQ/1648/2014 and UID/QUI/00100/2013), is acknowledged. C.P. and S.G. acknowledge COST action CM1302.

■ REFERENCES

(1) Batten, S. R.; Neville, S. M.; Turner, D. R. *Coordination Polymers: Design, Analysis and Application*; Springer: New York, 2010.
(2) (a) MacGillivray, L. R.; Lukehart, C. M. *Metal−Organic Framework Materials*; John Wiley & Sons: New York, 2014. (b) Seyyedi, B. *Metal−Organic Frameworks: A New Class of Crystalline Porous Materials*; Lambert Academic Publishing: Saarbrücken, Germany, 2014.
(3) For example, see: (a) You, L.; Zong, W.; Xiong, G.; Ding, F.; Wang, S.; Ren, B.; Dragutan, I.; Dragutan, V.; Sun, Y. *Appl. Catal., A* **2016**, *511*, 1−10. (b) Timokhin, I.; Pettinari, C.; Marchetti, F.;

DOI: 10.1021/acs.inorgchem.5b02997
Inorg. Chem. XXXX, XXX, XXX−XXX

Pettinari, R.; Condello, F.; Galli, S.; Alegria, E. C. B. A.; Martins, L. M. D. R. S.; Pombeiro, A. J. L. *Cryst. Growth Des.* **2015**, *15*, 2303−2317. (c) Gupta, S.; Kirillova, M.; Guedes da Silva, M. F. C.; Pombeiro, A. J. L.; Kirillov, A. M. *Inorg. Chem.* **2013**, *52*, 8601−8611. (d) Kirillov, A. M.; Karabach, Y. Y.; Kirillova, M.; Haukka, M.; Pombeiro, A. J. L. *Cryst. Growth Des.* **2012**, *12*, 1069−1074.

(4) (a) Chughtai, A. H.; Ahmad, N.; Younus, H. A.; Laypkov, A.; Verpoort, F. *Chem. Soc. Rev.* **2015**, *44*, 6804−6849. (b) Liu, J.; Chen, L.; Cui, H.; Zhang, L.; Zhang, J.; Su, C.-Y. *Chem. Soc. Rev.* **2014**, *43*, 6011−6061. (c) Yoon, M.; Srirambalaji, R.; Kim, K. *Chem. Rev.* **2012**, *112*, 1196−1231. (d) Corma, A.; Garcia, H.; Llabrés i Xamena, F. X. *Chem. Rev.* **2010**, *110*, 4606−4655.

(5) (a) Han, S. S.; Choi, S.-H.; van Duin, A. C. T. *Chem. Commun.* **2010**, *46*, 5713−5715. (b) Low, J. J.; Benin, A. I.; Jakubczak, P.; Abrahamian, J. F.; Faheem, S. A.; Willis, R. R. *J. Am. Chem. Soc.* **2009**, *131*, 15834−15842. (c) Greathouse, J. A.; Allendorf, M. D. *J. Am. Chem. Soc.* **2006**, *128*, 10678−10679.

(6) Bosch, M.; Zhang, M.; Zhou, H.-C. *Advances in Chemistry* **2014**, 1.

(7) Zhang, J.-P.; Zhang, Y.-B.; Lin, J.-B.; Chen, X.-M. *Chem. Rev.* **2012**, *112*, 1001−1033.

(8) For example, see: (a) Tabacaru, A.; Galli, S.; Pettinari, C.; Masciocchi, N.; McDonald, T. M.; Long, J. R. *CrystEngComm* **2015**, *17*, 4992−5001. (b) Galli, S.; Maspero, A.; Giacobbe, C.; Palmisano, G.; Nardo, L.; Comotti, A.; Bassanetti, I.; Sozzani, P.; Masciocchi, N. *J. Mater. Chem. A* **2014**, *2*, 12208−12221. (c) Tabacaru, A.; Pettinari, C.; Marchetti, F.; Galli, S.; Masciocchi, N. *Cryst. Growth Des.* **2014**, *14*, 3142−3152. (d) Padial, N. M.; Quartapelle Procopio, E.; Montoro, C.; López, E.; Oltra, J. E.; Colombo, V.; Maspero, A.; Masciocchi, N.; Galli, S.; Senkovska, I.; Kaskel, S.; Barea, E.; Navarro, J. A. R. *Angew. Chem., Int. Ed.* **2013**, *52*, 8290−8294. (e) Tabacaru, A.; Pettinari, C.; Timokhin, I.; Marchetti, F.; Carrasco-Marín, F.; Maldonado-Hódar, F. J.; Galli, S.; Masciocchi, N. *Cryst. Growth Des.* **2013**, *13*, 3087−3097. (f) Quartapelle Procopio, E.; Rojas, S.; Padial, N. M.; Galli, S.; Masciocchi, N.; Linares, F.; Miguel, D.; Oltra, J. E.; Navarro, J. A. R.; Barea, E. *Chem. Commun.* **2011**, *47*, 11751−11753.

(9) Colombo, V.; Galli, S.; Choi, H. J.; Han, G. D.; Maspero, A.; Palmisano, G.; Masciocchi, N.; Long, J. R. *Chem. Sci.* **2011**, *2*, 1311−1319.

(10) Pettinari, C.; Tabacaru, A.; Galli, S. *Coord. Chem. Rev.* **2016**, *307*, 1−31.

(11) Heering, C.; Boldog, I.; Vasylyeva, V.; Sanchiz, J.; Janiak, C. *CrystEngComm* **2013**, *15*, 9757−9768.

(12) For example, see: (a) Quartapelle Procopio, E.; Linares, F.; Montoro, C.; Colombo, V.; Maspero, A.; Barea, E.; Navarro, J. A. R. *Angew. Chem., Int. Ed.* **2010**, *49*, 7308−7311. (b) Montoro, C.; Linares, F.; Quartapelle Procopio, E.; Senkovska, I.; Kaskel, S.; Galli, S.; Masciocchi, N.; Barea, E.; Navarro, J. A. R. *J. Am. Chem. Soc.* **2011**, *133*, 11888−11891. (c) Quartapelle Procopio, E.; Fukushima, T.; Barea, E.; Navarro, J. A. R.; Horike, S.; Kitagawa, S. *Chem. - Eur. J.* **2012**, *18*, 13117−13125. (d) Qi, X.-L.; Zhang, C.; Wang, B.-Y.; Xue, W.; He, C.-T.; Liu, S.-Y.; Zhang, W.-X.; Chen, X.-M. *CrystEngComm* **2013**, *15*, 9530−9536. (e) Padial, N. M.; Quartapelle Procopio, E.; Montoro, C.; López, E.; Oltra, J. E.; Colombo, V.; Maspero, A.; Masciocchi, N.; Galli, S.; Senkovska, I.; Kaskel, S.; Barea, E.; Navarro, J. A. R. *Angew. Chem., Int. Ed.* **2013**, *52*, 8290−8294. (f) Kongpatpanich, K.; Horike, S.; Sugimoto, M.; Fukushima, T.; Umeyama, D.; Tsutsumi, Y.; Kitagawa, S. *Inorg. Chem.* **2014**, *53*, 9870−9875.

(13) For example, see: (a) Gao, W.-Y.; Yan, W.; Cai, R.; Meng, L.; Salas, A.; Wang, X.-S.; Wojtas, L.; Shi, X.; Ma, S. *Inorg. Chem.* **2012**, *51*, 4423−4425. (b) Lincke, J.; Lässig, D.; Kobalz, M.; Bergmann, J.; Handke, M.; Möllmer, J.; Lange, M.; Roth, C.; Möller, A.; Staudt, R.; Krautscheid, H. *Inorg. Chem.* **2012**, *51*, 7579−7586. (c) Gao, W.-Y.; Cai, R.; Meng, L.; Wojtas, L.; Zhou, W.; Yildirim, T.; Shi, X.; Ma, S. *Chem. Commun.* **2013**, *49*, 10516−10518. (d) Wang, L.; Ye, Y.; Zhang, L.; Chen, Q.; Ma, X.; Zhang, Z.; Xiang, S. *Inorg. Chem. Commun.* **2015**, *60*, 19−22. (e) Hou, J.-J.; Xu, X.; Jiang, N.; Wu, Y.-Q.; Zhang, X.-M. *J. Solid State Chem.* **2015**, *223*, 73−78. (f) Zhu, A.-X.; Qiu, Z.-Z.; Yang, L.-B.; Fang, X.-D.; Chen, S.-J.; Xu, Q.-Q.; Li, Q.-X. *CrystEngComm* **2015**, *17*, 4787−4792.

(14) For example, see: (a) Zhang, Z.; Xiang, S.; Zheng, Q.; Rao, X.; Mondal, J. U.; Arman, H. D.; Qian, G.; Chen, B. *Cryst. Growth Des.* **2010**, *10*, 2372−2375. (b) Zhang, S.-M.; Chang, Z.; Hu, T.-L.; Bu, X.-H. *Inorg. Chem.* **2010**, *49*, 11581−11586. (c) Li, Y.; Zhong, X.-H.; Zheng, F.-K.; Wu, M.-F.; Liu, Z.-F.; Guo, G.-C. *Inorg. Chem. Commun.* **2011**, *14*, 407−410. (d) Calahorro, A. J.; Zaragoza, G.; Salinas-Castillo, A.; Seco, J. M.; Rodriguez-Dieguez, A. *Polyhedron* **2014**, *80*, 228−232. (e) Wu, M.-F.; Shen, T.-T.; He, S.; Wu, K.-Q.; Wang, S.-H.; Liu, Z.-F.; Zheng, F.-K.; Guo, G.-C. *CrystEngComm* **2015**, *17*, 7473−7476. (f) Ordonez, C.; Kinnibrugh, T. L.; Xu, H.; Lindline, J.; Timofeeva, T.; Wei, Q. *Crystals* **2015**, *5*, 193−205.

(15) For example, see: (a) Lu, W.-G.; Su, C.-Y.; Lu, T.-B.; Jiang, L.; Chen, J.-M. *J. Am. Chem. Soc.* **2006**, *128*, 34−35. (b) Lu, W.-G.; Jiang, L.; Feng, X.-L.; Lu, T.-B. *Cryst. Growth Des.* **2008**, *8*, 986−994. (c) Zhang, F.; Li, Z.; Ge, T.; Yao, H.; Li, G.; Lu, H.; Zhu, Y. *Inorg. Chem.* **2010**, *49*, 3776−3788. (d) Wang, W.-Y.; Yang, Z.-L.; Wang, C.-J.; Lu, H.-J.; Zang, S.-Q.; Li, G. *CrystEngComm* **2011**, *13*, 4895−4902. (e) Fan, R.-Q.; Wang, L.-Y.; Chen, H.; Zhou, G.-P.; Yang, Y.-L.; Hasi, W.; Cao, W.-W. *Polyhedron* **2012**, *33*, 90−96. (f) Chen, S.-S.; Liu, Q.; Zhao, Y.; Qiao, R.; Sheng, L.-Q.; Liu, Z.-D.; Yang, S.; Song, C.-F. *Cryst. Growth Des.* **2014**, *14*, 3727−3741.

(16) Lin, Q.; Meloni, D.; Pan, Y.; Xia, R.; Rodgers, J.; Shepard, S.; Li, M.; Galya, L.; Metcalf, B.; Yue, T.-N.; Liu, P.; Zhou, J. *Org. Lett.* **2009**, *11*, 1999−2002.

(17) Coelho, A. *J. Appl. Crystallogr.* **2003**, *36*, 86−95.

(18) *TOPAS*, version 3.0; Bruker AXS: Karlsruhe, Germany, 2005.

(19) To describe the ligand, the *z*-matrix formalism was used, imposing idealized bond distances (Å) and angles (deg) as follows: C−C, C−N, and N−N of the pentaatomic ring, 1.36; exocyclic C−C, refined in the range of 1.45−1.50; C−O, 1.25; N−H, 0.95; aliphatic C−H, 1.10; pentaatomic ring internal bond angles, 108; pentaatomic ring external bond angles, 126; O−C−O, 120; H−C−H, 109.5. In the case of **Cd-dmpzc**, to describe DMF, the *z*-matrix formalism was used, imposing idealized bond distances (Å) and angles (deg) as follows: C−N, refined in the range of 1.45−1.50; C−O, 1.25; C−H, 1.10; C−N−C, 120; N−C−O, 120; N−C−H_{ald}, 120; H−C−H, 109.5.

(20) Cheary, R. W.; Coelho, A. *J. Appl. Crystallogr.* **1992**, *25*, 109−121.

(21) Upon comparison of the TGA and VT-PXRD results, the reader must be aware that the thermocouple of the VT-PXRD setup is *not* in direct contact with the sample, thus determining a slight difference in the temperature at which the same event is detected by the two techniques. The TGA temperatures have to be considered more reliable.

(22) (a) Shul'pin, G. B. *J. Mol. Catal. A: Chem.* **2002**, *189*, 39−66. (b) Shul'pin, G. B. *C. R. Chim.* **2003**, *6*, 163−178. (c) Shul'pin, G. B. *Mini-Rev. Org. Chem.* **2009**, *6*, 95−104. (d) Shul'pin, G. B.; Kozlov, Y. N.; Shul'pina, L. S.; Kudinov, A. R.; Mandelli, D. *Inorg. Chem.* **2009**, *48*, 10480−10482. (e) Shul'pin, G. B.; Kozlov, Y. N.; Shul'pina, L. S.; Petrovskiy, P. V. *Appl. Organomet. Chem.* **2010**, *24*, 464−472. (f) Shul'pin, G. B. *Dalton Trans.* **2013**, *42*, 12794−12818.

(23) (a) Kopylovich, M. N.; Mizar, A.; Guedes da Silva, M. F. C.; Mac Leod, T. C. O.; Mahmudov, K. T.; Pombeiro, A. J. L. *Chem. - Eur. J.* **2013**, *19*, 588−600. (b) Pettinari, C.; Marchetti, F.; Cerquetella, A.; Pettinari, R.; Monari, M.; Mac Leod, T. C. O.; Martins, L. M. D. R. S.; Pombeiro, A. J. L. *Organometallics* **2011**, *30*, 1616−1626. (c) Naïli, H.; Hajlaoui, F.; Mhiri, T.; Mac Leod, T. C. O.; Kopylovich, M. N.; Mahmudov, K. T.; Pombeiro, A. J. L. *Dalton Trans.* **2013**, *42*, 399−406. (d) Shixaliyev, N. Q.; Maharramov, A. M.; Gurbanov, A. V.; Nenajdenko, V. G.; Muzalevskiy, V. M.; Mahmudov, K. T.; Kopylovich, M. N. *Catal. Today* **2013**, *217*, 76−79. (e) Nkhili, N. L.; Rekik, W.; Mhiri, T.; Mahmudov, K. T.; Kopylovich, M. N.; Naïli, H. *Inorg. Chim. Acta* **2014**, *412*, 27−31. (f) Mahmudov, K. T.; Kopylovich, M. N.; Haukka, M.; Mahmudova, G. S.; Esmaeila, E. F.; Chyragov, F. M.; Pombeiro, A. J. L. *J. Mol. Struct.* **2013**, *1048*, 108−112. (g) Rocha, B. G. M.; Mac Leod, T. C. O.; Guedes da Silva, M. F.

DOI: 10.1021/acs.inorgchem.5b02997
Inorg. Chem. XXXX, XXX, XXX−XXX

C.; Luzyanin, K. V.; Martins, L. M. D. R. S.; Pombeiro, A. J. L. *Dalton Trans.* **2014**, *43*, 15192−15200.
(24) Bulbule, V. J.; Deshpande, V. H.; Velu, S.; Sudalai, A.; Sivasankar, S.; Sathe, V. T. *Tetrahedron* **1999**, *55*, 9325−9332.
(25) Chay, R. S.; Luzyanin, K. V.; Kukushkin, V. Y.; Guedes da Silva, M. F. C.; Pombeiro, A. J. L. *Organometallics* **2012**, *31*, 2379−2387.
(26) Deng, H.; Doonan, C. J.; Furukawa, H.; Ferreira, R. B.; Towne, J.; Knobler, C. B.; Wang, B.; Yaghi, O. M. *Science* **2010**, *327*, 846−850.
(27) Nakamoto, K. *Infrared and Raman spectra of inorganic and coordination compounds, Part B*, 6th ed.; Wiley: New York, 2009.
(28) The two strong bands lying in the ranges of 1549−1486 and 1428−1377 cm^{-1} correspond to the asymmetric (ν_a) and symmetric (ν_s) stretching of the carboxylate anion, respectively. Their difference, $\Delta\nu = \nu_a - \nu_s$ = 141−173 cm^{-1}, indicates a μ_2-coordination geometry. On the other hand, the presence of water and DMF is witnessed, respectively, by the broad band lying in the range of 3100−3600 cm^{-1} and by the strong band peaking in the range of 1655−1678 cm^{-1}.
(29) On the basis of the IR spectrum of the free ligand (Figure S2), the band peaking at 3195 cm^{-1} in the spectrum of **Pd-dmpzc** can be ascribed to the N−H stretching of pyrazole, while the very strong band at 1683 cm^{-1} is due to the C═O stretching of a neutral carboxylic group. In addition, the presence of a very broad band in the range of 3200−2400 cm^{-1} can be ascribed to the superposition of the aliphatic C−H stretching with the O−H stretching of hydrogen-bonded carboxylic groups (Silverstein, R. M.; Webster, F. X.; Kiemle, D. J. *Spectrometric identification of organic compounds*, 7th ed.; Wiley: New York, 2005).
(30) The concomitant presence of a band at 3171 cm^{-1}, ascribed to N−H stretching, and the absence of bands retraceable to O−H stretching, originally present in the IR spectrum of the free ligand (Figure S2), confirm the partial deprotonation of the ligand. In addition, the two strong bands at 1586 and 1373 cm^{-1} correspond to the asymmetric (ν_a) and symmetric (ν_s) stretching of the carboxylate anion, respectively. Their difference, $\Delta\nu = \nu_a - \nu_s$ = 213 cm^{-1}, likely indicates a monodentate coordination geometry.[27]
(31) In more detail, both spacers are N,O-chelating versus one metal ion and coordinate the nearby one through the remaining oxygen atom.
(32) Calculated with *PLATON*: Spek, A. L. *J. Appl. Crystallogr.* **2003**, *36*, 7−13.
(33) Batsanov, S. S. *Inorg. Mater.* **2001**, *37*, 871−885.
(34) In detail, *a*, *b*, *c*, and β increase by 0.5, 0.4, 0.2, and 0.02%, respectively.
(35) In detail, *a*, *b*, *c*, and β increase by 0.4, 0.6, 2.9, and 1.0%, respectively.
(36) In detail, *a*, *b*, and *c* increase by 0.2, 0.2, and 0.8%, respectively.
(37) For example, see: (a) Sutradhar, M.; Martins, L. M. D. R. S.; Guedes da Silva, M. F. C.; Pombeiro, A. J. L. *Coord. Chem. Rev.* **2015**, *301−302*, 200−239. (b) Sutradhar, M.; Martins, L. M. D. R. S.; Guedes da Silva, M. F. C.; Mahmudov, K. T.; Liu, C.-M.; Pombeiro, A. J. L. *Eur. J. Inorg. Chem.* **2015**, 3959−3969. (c) Zaltariov, M.-F.; Alexandru, M.; Cazacu, M.; Shova, S.; Novitchi, G.; Train, C.; Dobrov, A.; Kirillova, M. V.; Alegria, E. C. B. A.; Pombeiro, A. J. L.; Arion, V. B. *Eur. J. Inorg. Chem.* **2014**, *29*, 4946−4956. (d) Martins, L. M. D. R. S.; Pombeiro, A. J. L. *Coord. Chem. Rev.* **2014**, *265*, 74−88. (e) Silva, T. F. S.; Martins, L. M. D. R. S.; Guedes da Silva, M. F.; Kuznetsov, M. L.; Fernandes, A. R.; Silva, A.; Santos, S.; Pan, C.-J.; Lee, J.-F.; Hwang, B.-J.; Pombeiro, A. J. L. *Chem. - Asian J.* **2014**, *9*, 1132−1143. (f) Martins, L. M. D. R. S.; Martins, A.; Alegria, E. C. B. A.; Carvalho, A. P.; Pombeiro, A. J. L. *Appl. Catal., A* **2013**, *464−465*, 43−50. (g) Sutradhar, M.; Kirillova, M. V.; Guedes da Silva, M. F. C.; Martins, L. M. D. R. S.; Pombeiro, A. J. L. *Inorg. Chem.* **2012**, *51*, 11229−11231. (h) Silva, T. F. S.; Martins, L. M. D. R. S.; Guedes da Silva, M. F.; Fernandes, A. R.; Silva, A.; Borralho, P. M.; Santos, S.; Rodrigues, C. M. P.; Pombeiro, A. J. L. *Dalton Trans.* **2012**, *41*, 12888−12897.
(38) Fernandes, R. R.; Lasri, J.; Guedes da Silva, M. F. C.; da Silva, J. A. L.; Fraústo da Silva, J. J. R.; Pombeiro, A. J. L. *Appl. Catal., A* **2011**, *402*, 110−120.
(39) Fernandes, R. R.; Lasri, J.; Kirillov, A. M.; Guedes da Silva, M. F. C.; da Silva, J. A. L.; Fraústo da Silva, J. J. R.; Pombeiro, A. J. L. *Eur. J. Inorg. Chem.* **2011**, 3781−3790.
(40) (a) Di Nicola, C.; Garau, F.; Karabach, Y. Y.; Martins, L. M. D. R. S.; Monari, M.; Pandolfo, L.; Pettinari, C.; Pombeiro, A. J. L. *Eur. J. Inorg. Chem.* **2009**, 666−676. (b) Kopylovich, M. N.; Nunes, A. C. C.; Mahmudov, K. T.; Haukka, M.; Mac Leod, T. C. O.; Martins, L. M. D. R. S.; Kuznetsov, M. L.; Pombeiro, A. J. L. *Dalton Trans.* **2011**, *40*, 2822−2836. (c) Contaldi, S.; Di Nicola, C.; Garau, F.; Karabach, Y. Y.; Martins, L. M. D. R. S.; Monari, M.; Pandolfo, L.; Pettinari, C.; Pombeiro, A. J. L. *Dalton Trans.* **2009**, 4928−4941.
(41) For example, see: (a) Sutradhar, M.; Martins, L. M. D. R. S.; Guedes da Silva, M. F. C.; Alegria, E. C. B. A.; Liu, C.-M.; Pombeiro, A. J. L. *Dalton Trans.* **2014**, *43*, 3966−3977. (b) Karabach, Y. Y.; Kopylovich, M. N.; Mahmudov, K. T.; Pombeiro, A. J. L. Microwave-assisted catalytic oxidation of alcohols to carbonyl compounds. In *Advances in Organometallic Chemistry and Catalysis*; Pombeiro, A. J. L., Ed.; Wiley-VCH: Weinheim, Germany, 2013; Chapter 22, pp 285−294.
(42) For example, see: (a) Karmakar, A.; Martins, L. M. D. R. S.; Guedes da Silva, M. F. C.; Hazra, S.; Pombeiro, A. J. L. *Catal. Lett.* **2015**, *145*, 2066−2076. (b) Alexandru, M.; Cazacu, M.; Arvinte, A.; Shova, S.; Turta, C.; Simionescu, B. C.; Dobrov, A.; Alegria, E. C. B. A.; Martins, L. M. D. R. S.; Pombeiro, A. J. L.; Arion, B. *Eur. J. Inorg. Chem.* **2014**, 120−131. (c) Sabbatini, A.; Martins, L. M. D. R. S.; Mahmudov, K. T.; Kopylovich, M. N.; Drew, M. G. B.; Pettinari, C.; Pombeiro, A. J. L. *Catal. Commun.* **2014**, *48*, 4048−4058. (d) Sutradhar, M.; Martins, L. M. D. R. S.; Guedes da Silva, M. F. C.; Pombeiro, A. J. L. *Appl. Catal., A* **2015**, *493*, 50−57. (e) Kopylovich, M. N.; Ribeiro, A. P. C.; Alegria, E. C. B. A.; Martins, N. M. R.; Martins, L. M. D. R. S.; Pombeiro, A. J. L. *Adv. Organomet. Chem.* **2015**, *63*, 91−174. (f) Ma, Z.; Shi, H.; Deng, X.; Guedes da Silva, M. F. C.; Martins, L. M. D. R. S.; Pombeiro, A. J. L. *Dalton Trans.* **2015**, *44*, 1388−1396.
(43) (a) Feldberg, L.; Sasson, Y. *Tetrahedron Lett.* **1996**, *37*, 2063−2066. (b) Mahdavi, V.; Mardani, M. J. *J. Chem. Sci.* **2012**, *124*, 1107−1115.
(44) (a) Shibasaki, M.; Kanai, M.; Matsunaga, S. Bifunctional Molecular Catalysis. In *Topics in Organometallic Chemistry*; Kariya, T., Shibasaki, M., Eds.; Springer: Heidelberg, Germany, 2011; Vol. *37*, Chapter 3, p 12. (b) Palomo, C.; Oiarbide, M.; Mielgo, A. *Angew. Chem., Int. Ed.* **2004**, *43*, 5442−5444.
(45) For example, see: (a) Qi, N.; Liao, R.-Z.; Yu, J.-G.; Liu, R.-Z. *J. Comput. Chem.* **2009**, *31*, 1376−1384. (b) Liu, S.; Wolf, C. *Org. Lett.* **2008**, *10*, 1831−1834. (c) Qin, B.; Xiao, X.; Liu, X.; Huang, J.; Wen, Y.; Feng, X. *J. Org. Chem.* **2007**, *72*, 9323−9328.

DOI: 10.1021/acs.inorgchem.5b02997
Inorg. Chem. XXXX, XXX, XXX−XXX